

Kim, S.E et. al “An Innovative Design For Steel Frame Using Advanced Analysis<sup>footnotemark</sup>”  
*Structural Engineering Handbook*  
Ed. Chen Wai-Fah  
Boca Raton: CRC Press LLC, 1999

# An Innovative Design For Steel Frame Using Advanced Analysis<sup>1</sup>

---

## 28.1 Introduction

## 28.2 Practical Advanced Analysis

Second-Order Refined Plastic Hinge Analysis • Analysis of Semi-Rigid Frames • Geometric Imperfection Methods • Numerical Implementation

## 28.3 Verifications

Axially Loaded Columns • Portal Frame • Six-Story Frame • Semi-Rigid Frame

## 28.4 Analysis and Design Principles

Design Format • Loads • Load Combinations • Resistance Factors • Section Application • Modeling of Structural Members • Modeling of Geometric Imperfection • Load Application • Analysis • Load-Carrying Capacity • Serviceability Limits • Ductility Requirements • Adjustment of Member Sizes

## 28.5 Computer Program

Program Overview • Hardware Requirements • Execution of Program • Users' Manual

## 28.6 Design Examples

Roof Truss • Unbraced Eight-Story Frame • Two-Story Four-Bay Semi-Rigid Frame

## 28.7 Defining Terms

## References

## Further Reading

Seung-Eock Kim  
Department of Civil Engineering,  
Sejong University,  
Seoul, South Korea

W. F. Chen  
School of Civil Engineering,  
Purdue University,  
West Lafayette, IN

## 28.1 Introduction

---

The steel design methods used in the U.S. are allowable stress design (ASD), plastic design (PD), and load and resistance factor design (LRFD). In ASD, the stress computation is based on a first-order elastic analysis, and the geometric nonlinear effects are implicitly accounted for in the member design equations. In PD, a first-order plastic-hinge analysis is used in the structural analysis. PD allows inelastic force redistribution throughout the structural system. Since geometric nonlinearity and gradual yielding effects are not accounted for in the analysis of plastic design, they are approximated

---

<sup>1</sup>The material in this chapter was previously published by CRC Press in *LRFD Steel Design Using Advanced Analysis*, W. F. Chen and Seung-Eock Kim, 1997.

in member design equations. In LRFD, a first-order elastic analysis with amplification factors or a direct second-order elastic analysis is used to account for geometric nonlinearity, and the ultimate strength of **beam-column** members is implicitly reflected in the design interaction equations. All three design methods require separate member capacity checks including the calculation of the K factor. In the following, the characteristics of the LRFD method are briefly described.

The strength and stability of a structural system and its members are related, but the interaction is treated separately in the current American Institute of Steel Construction (AISC)-LRFD specification [2]. In current practice, the interaction between the structural system and its members is represented by the effective length factor. This aspect is described in the following excerpt from SSRC Technical Memorandum No. 5 [28]:

Although the maximum strength of frames and the maximum strength of component members are interdependent (but not necessarily coexistent), it is recognized that in many structures it is not practical to take this interdependence into account rigorously. At the same time, it is known that difficulties are encountered in complex frameworks when attempting to compensate automatically in **column** design for the instability of the entire frame (for example, by adjustment of column effective length). Therefore, SSRC recommends that, in design practice, the two aspects, stability of separate members and elements of the structure and stability of the structure as a whole, be considered separately.

This design approach is marked in Figure 28.1 as the indirect analysis and design method.

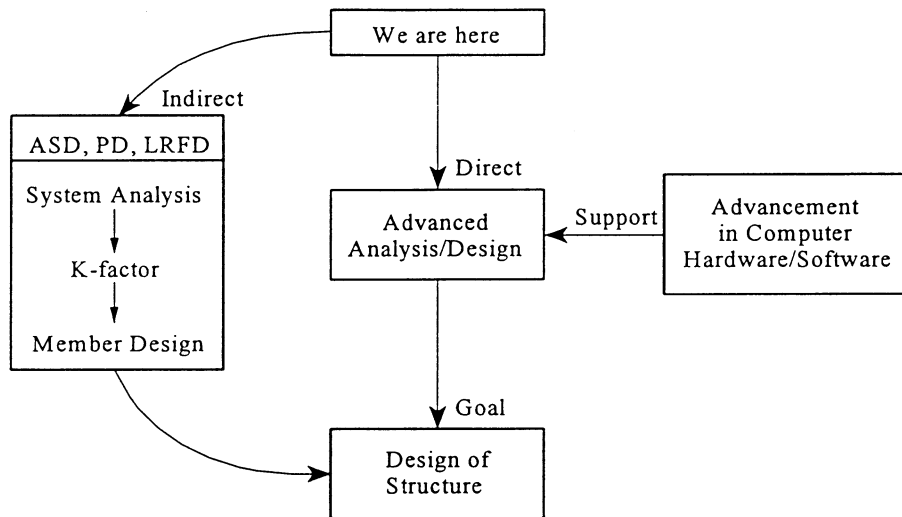


FIGURE 28.1: Analysis and design methods.

In the current AISC-LRFD specification [2], first-order elastic analysis or second-order elastic analysis is used to analyze a structural system. In using first-order elastic analysis, the first-order moment is amplified by  $B_1$  and  $B_2$  factors to account for second-order effects. In the specification, the members are isolated from a structural system, and they are then designed by the member strength curves and interaction equations as given by the specifications, which implicitly account for second-order effects, inelasticity, residual stresses, and **geometric imperfections** [8]. The column

curve and beam curve were developed by a curve-fit to both theoretical solutions and experimental data, while the beam-column interaction equations were determined by a curve-fit to the so-called “exact” plastic-zone solutions generated by Kanchanlai [14].

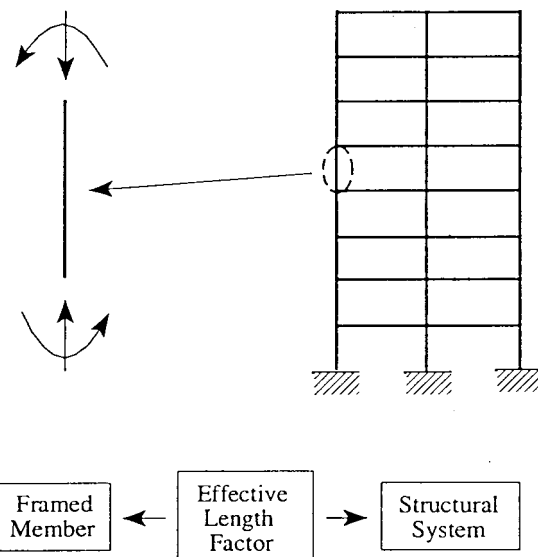


FIGURE 28.2: Interaction between a structural system and its component members.

In order to account for the influence of a structural system on the strength of individual members, the effective length factor is used, as illustrated in Figure 28.2. The effective length method generally provides a good design of framed structures. However, several difficulties are associated with the use of the effective length method, as follows:

1. The effective length approach cannot accurately account for the interaction between the structural system and its members. This is because the interaction in a large structural system is too complex to be represented by the simple effective length factor  $K$ . As a result, this method cannot accurately predict the actual required strengths of its framed members.
2. The effective length method cannot capture the inelastic redistributions of internal forces in a structural system, since the first-order elastic analysis with  $B_1$  and  $B_2$  factors accounts only for second-order effects but not the inelastic redistribution of internal forces. The effective length method provides a conservative estimation of the ultimate load-carrying capacity of a large structural system.
3. The effective length method cannot predict the failure modes of a structural system subject to a given load. This is because the LRFD interaction equation does not provide any information about failure modes of a structural system at the **factored loads**.
4. The effective length method is not user friendly for a computer-based design.
5. The effective length method requires a time-consuming process of separate member capacity checks involving the calculation of  $K$  factors.

With the development of computer technology, two aspects, the stability of separate members and the stability of the structure as a whole, can be treated rigorously for the determination of the maximum strength of the structures. This design approach is marked in Figure 28.1 as the direct analysis and design method. The development of the direct approach to design is called **advanced analysis**, or more specifically, second-order inelastic analysis for frame design. In this direct approach, there is no need to compute the effective length factor, since separate member capacity checks encompassed by the specification equations are not required. With the current available computing technology, it is feasible to employ advanced analysis techniques for direct frame design. This method has been considered impractical for design office use in the past. The purpose of this chapter is to present a practical, direct method of steel frame design, using advanced analysis, that will produce almost identical member sizes as those of the LRFD method.

The advantages of advanced analysis in design use are outlined as follows:

1. Advanced analysis is another tool for structural engineers to use in steel design, and its adoption is not mandatory but will provide a flexibility of options to the designer.
2. Advanced analysis captures the **limit state** strength and stability of a structural system and its individual members directly, so separate member capacity checks encompassed by the specification equations are not required.
3. Compared to the LRFD and ASD, advanced analysis provides more information of structural behavior by direct inelastic **second-order analysis**.
4. Advanced analysis overcomes the difficulties due to incompatibility between the elastic global analysis and the limit state member design in the conventional LRFD method.
5. Advanced analysis is user friendly for a computer-based design, but the LRFD and ASD are not, since they require the calculation of K factor on the way from their analysis to separate member capacity checks.
6. Advanced analysis captures the inelastic redistribution of internal forces throughout a structural system, and allows an economic use of material for highly indeterminate steel frames.
7. It is now feasible to employ advanced analysis techniques that have been considered impractical for design office use in the past, since the power of personal computers and engineering workstations is rapidly increasing.
8. Member sizes determined by advanced analysis are close to those determined by the LRFD method, since the advanced analysis method is calibrated against the LRFD column curve and beam-column interaction equations. As a result, advanced analysis provides an alternative to the LRFD.
9. Advanced analysis is time effective since it completely eliminates tedious and often confused member capacity checks, including the calculation of K factors in the LRFD and ASD.

Among various advanced analyses, including plastic-zone, quasi-plastic hinge, elastic-plastic hinge, notional-load plastic-hinge, and refined **plastic hinge** methods, the refined plastic hinge method is recommended, since it retains the efficiency and simplicity of computation and accuracy for practical use. The method is developed by imposing simple modifications on the conventional elastic-plastic hinge method. These include a simple modification to account for the gradual sectional **stiffness** degradation at the plastic hinge locations and to include the gradual member stiffness degradation between two plastic hinges.

The key considerations of the conventional LRFD method and the practical advanced analysis method are compared in Table 28.1. While the LRFD method does account for key behavioral effects implicitly in its column strength and beam-column interaction equations, the advanced anal-

ysis method accounts for these effects explicitly through **stability functions**, stiffness degradation functions, and geometric imperfections, to be discussed in detail in Section 28.2.

**TABLE 28.1** Key Considerations of Load and Resistance Factor Design (LRFD) and Proposed Methods

Key consideration	LRFD	Proposed method
Second-order effects	Column curve $B_1, B_2$ factor	Stability function
Geometric imperfection	Column curve	Explicit imperfection modeling method $\psi = 1/500$ for unbraced frame $\delta_c = L_c/1000$ for braced frame Equivalent notional load method $\alpha = 0.002$ for unbraced frame $\alpha = 0.004$ for braced frame Further reduced tangent modulus method $E'_t = 0.85 E_t$
Stiffness degradation associated with residual stresses	Column curve	CRC tangent modulus
Stiffness degradation associated with flexure	Column curve Interaction equations	Parabolic degradation function
Connection nonlinearity	No procedure	Power model/rotational spring

Advanced analysis holds many answers to real behavior of steel structures and, as such, we recommend the proposed design method to engineers seeking to perform frame design in efficiency and rationality, yet consistent with the present LRFD specification. In the following sections, we will present a practical advanced analysis method for the design of steel frame structures with LRFD. The validity of the approach will be demonstrated by comparing case studies of actual members and frames with the results of analysis/design based on exact plastic-zone solutions and LRFD designs. The wide range of case studies and comparisons should confirm the validity of this advanced method.

## 28.2 Practical Advanced Analysis

This section presents a practical advanced analysis method for the direct design of steel frames by eliminating separate member capacity checks by the specification. The refined plastic hinge method was developed and refined by simply modifying the conventional elastic-plastic hinge method to achieve both simplicity and a realistic representation of actual behavior [15, 25]. Verification of the method will be given in the next section to provide final confirmation of the validity of the method.

Connection flexibility can be accounted for in advanced analysis. Conventional analysis and design of steel structures are usually carried out under the assumption that beam-to-column connections are either fully rigid or ideally pinned. However, most connections in practice are semi-rigid and their behavior lies between these two extreme cases. In the AISC-LRFD specification [2], two types of construction are designated: Type FR (fully restrained) construction and Type PR (partially restrained) construction. The LRFD specification permits the evaluation of the flexibility of connections by "rational means".

Connection behavior is represented by its moment-rotation relationship. Extensive experimental work on connections has been performed, and a large body of moment-rotation data collected. With this data base, researchers have developed several connection models, including linear, polynomial, B-spline, power, and exponential. Herein, the three-parameter power model proposed by Kishi and Chen [21] is adopted.

Geometric imperfections should be modeled in frame members when using advanced analysis. Geometric imperfections result from unavoidable error during fabrication or erection. For structural members in building frames, the types of geometric imperfections are out-of-straightness and out-of-

plumbness. Explicit modeling and equivalent **notional loads** have been used to account for geometric imperfections by previous researchers. In this section, a new method based on further reduction of the tangent stiffness of members is developed [15, 16]. This method provides a simple means to account for the effect of imperfection without inputting notional loads or explicit geometric imperfections.

The practical advanced analysis method described in this section is limited to two-dimensional braced, unbraced, and semi-rigid frames subject to static loads. The spatial behavior of frames is not considered, and lateral torsional buckling is assumed to be prevented by adequate lateral bracing. A compact W section is assumed so sections can develop full plastic moment capacity without local buckling. Both strong- and weak-axis bending of wide flange sections have been studied using the practical advanced analysis method [15]. The method may be considered an interim analysis/design procedure between the conventional LRFD method widely used now and a more rigorous advanced analysis/design method such as the plastic-zone method to be developed in the future for practical use.

### 28.2.1 Second-Order Refined Plastic Hinge Analysis

In this section, a method called the refined plastic hinge approach is presented. This method is comparable to the elastic-plastic hinge analysis in efficiency and simplicity, but without its limitations. In this analysis, stability functions are used to predict second-order effects. The benefit of stability functions is that they make the analysis method practical by using only one element per beam-column. The **refined plastic hinge analysis** uses a two-surface yield model and an effective tangent modulus to account for stiffness degradation due to distributed plasticity in framed members. The member stiffness is assumed to degrade gradually as the second-order forces at critical locations approach the cross-section plastic strength. Column tangent modulus is used to represent the effective stiffness of the member when it is loaded with a high axial load. Thus, the refined plastic hinge model approximates the effect of distributed plasticity along the element length caused by initial imperfections and large bending and axial force actions. In fact, research by Liew et al. [25, 26], Kim and Chen [16], and Kim [15] has shown that refined plastic hinge analysis captures the interaction of strength and stability of structural systems and that of their component elements. This type of analysis method may, therefore, be classified as an advanced analysis and separate specification member capacity checks are not required.

#### Stability Function

To capture second-order effects, stability functions are recommended since they lead to large savings in modeling and solution efforts by using one or two elements per member. The simplified stability functions reported by Chen and Lui [7] or an alternative may be used. Considering the prismatic beam-column element, the incremental force-displacement relationship of this element may be written as

$$\begin{bmatrix} \dot{M}_A \\ \dot{M}_B \\ \dot{P} \end{bmatrix} = \frac{EI}{L} \begin{bmatrix} S_1 & S_2 & 0 \\ S_2 & S_1 & 0 \\ 0 & 0 & A/I \end{bmatrix} \begin{bmatrix} \dot{\theta}_A \\ \dot{\theta}_B \\ \dot{e} \end{bmatrix} \quad (28.1)$$

where

- $S_1, S_2$  = stability functions
- $\dot{M}_A, \dot{M}_B$  = incremental end moment
- $\dot{P}$  = incremental axial force
- $\dot{\theta}_A, \dot{\theta}_B$  = incremental joint rotation
- $\dot{e}$  = incremental axial displacement
- $A, I, L$  = area, moment of inertia, and length of beam-column element
- $E$  = modulus of elasticity.

In this formulation, all members are assumed to be adequately braced to prevent out-of-plane buckling, and their cross-sections are compact to avoid local buckling.

### Cross-Section Plastic Strength

Based on the AISC-LRFD bilinear interaction equations [2], the cross-section plastic strength may be expressed as Equation 28.2. These AISC-LRFD cross-section plastic strength curves may be adopted for both strong- and weak-axis bending (Figure 28.3).

$$\frac{P}{P_y} + \frac{8}{9} \frac{M}{M_p} = 1.0 \text{ for } \frac{P}{P_y} \geq 0.2 \quad (28.2a)$$

$$\frac{P}{P_y} + \frac{M}{M_p} = 1.0 \text{ for } \frac{P}{P_y} < 0.2 \quad (28.2b)$$

where

$P, M$  = second-order axial force and bending moment

$P_y$  = squash load

$M_p$  = plastic moment capacity

### CRC Tangent Modulus

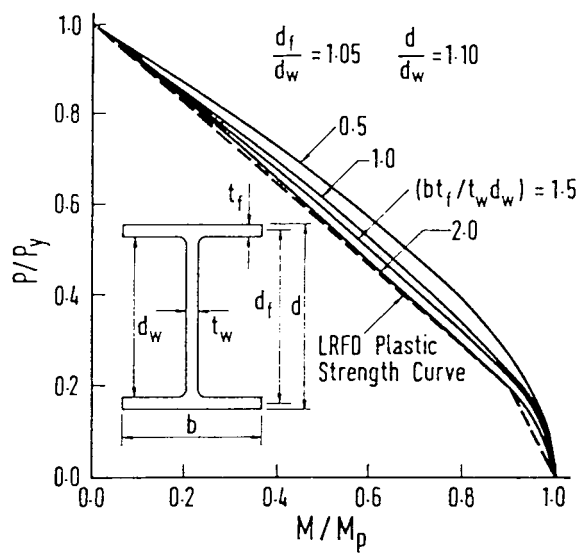
The CRC tangent modulus concept is employed to account for the gradual yielding effect due to residual stresses along the length of members under axial loads between two plastic hinges. In this concept, the elastic modulus,  $E$ , instead of moment of inertia,  $I$ , is reduced to account for the reduction of the elastic portion of the cross-section since the reduction of elastic modulus is easier to implement than that of moment of inertia for different sections. The reduction rate in stiffness between the weak and strong axis is different, but this is not considered here. This is because rapid degradation in stiffness in the weak-axis strength is compensated well by the stronger weak-axis plastic strength. As a result, this simplicity will make the present methods practical. From Chen and Lui [7], the CRC  $E_t$  is written as (Figure 28.4):

$$E_t = 1.0E \text{ for } P \leq 0.5P_y \quad (28.3a)$$

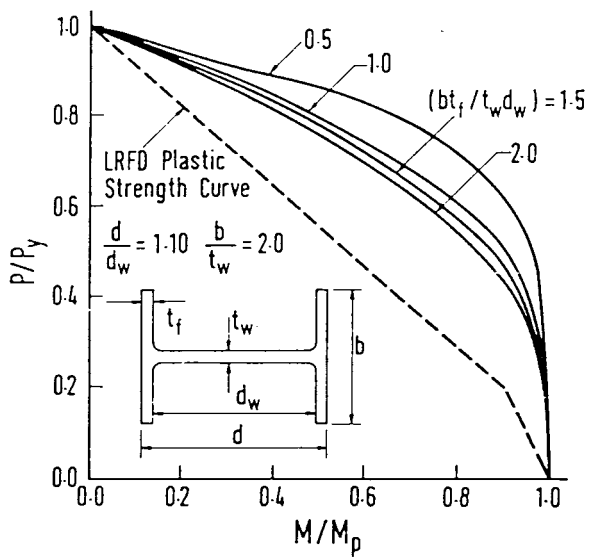
$$E_t = 4 \frac{P}{P_y} E \left( 1 - \frac{P}{P_y} \right) \text{ for } P > 0.5P_y \quad (28.3b)$$

### Parabolic Function

The tangent modulus model in Equation 28.3 is suitable for  $P/P_y > 0.5$ , but it is not sufficient to represent the stiffness degradation for cases with small axial forces and large bending moments. A gradual stiffness degradation of plastic hinge is required to represent the distributed plasticity effects associated with bending actions. We shall introduce the hardening plastic hinge model to represent the gradual transition from elastic stiffness to zero stiffness associated with a fully developed plastic hinge. When the hardening plastic hinges are present at both ends of an element, the incremental force-displacement relationship may be expressed as [24]:



(a)



(b)

FIGURE 28.3: Strength interaction curves for wide-flange sections.

$$\begin{bmatrix} \dot{M}_A \\ \dot{M}_B \\ \dot{P} \end{bmatrix} = \frac{E_t I}{L} \begin{bmatrix} \eta_A \left[ S_1 - \frac{S_2^2}{S_1} (1 - \eta_B) \right] & \eta_A \eta_B S_2 & 0 \\ \eta_A \eta_B S_2 & \eta_B \left[ S_1 - \frac{S_2^2}{S_1} (1 - \eta_A) \right] & 0 \\ 0 & 0 & A/I \end{bmatrix} \begin{bmatrix} \dot{\theta}_A \\ \dot{\theta}_B \\ \dot{e} \end{bmatrix} \quad (28.4)$$

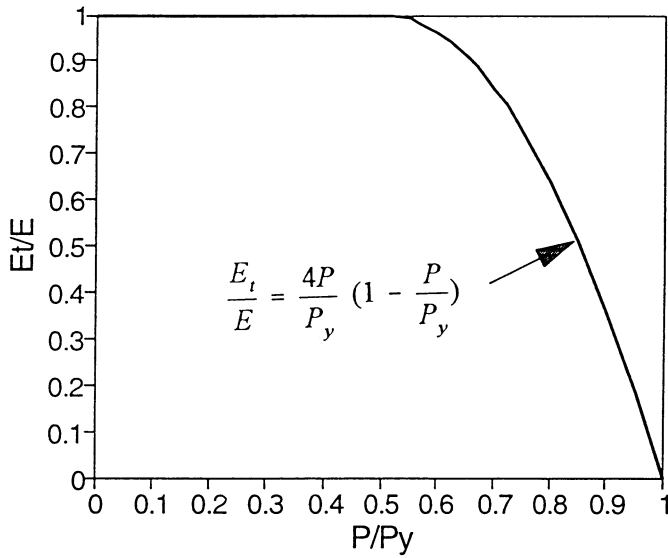


FIGURE 28.4: Member tangent stiffness degradation derived from the CRC column curve.

where

$\dot{M}_A, \dot{M}_B, \dot{P}$  = incremental end moments and axial force, respectively

$S_1, S_2$  = stability functions

$E_t$  = tangent modulus

$\eta_A, \eta_B$  = element stiffness parameters

The parameter  $\eta$  represents a gradual stiffness reduction associated with flexure at sections. The partial plastification at cross-sections in the end of elements is denoted by  $0 < \eta < 1$ . The  $\eta$  may be assumed to vary according to the parabolic expression (Figure 28.5):

$$\eta = 4\alpha(1 - \alpha) \text{ for } \alpha > 0.5 \quad (28.5)$$

where  $\alpha$  is the force state parameter obtained from the limit state surface corresponding to the element end (Figure 28.6):

$$\alpha = \frac{P}{P_y} + \frac{8}{9} \frac{M}{M_p} \text{ for } \frac{P}{P_y} \geq \frac{2}{9} \frac{M}{M_p} \quad (28.6a)$$

$$\alpha = \frac{P}{2P_y} + \frac{M}{M_p} \text{ for } \frac{P}{P_y} < \frac{2}{9} \frac{M}{M_p} \quad (28.6b)$$

where

$P, M$  = second-order axial force and bending moment at the cross-section

$M_p$  = plastic moment capacity

### 28.2.2 Analysis of Semi-Rigid Frames

#### Practical Connection Modeling

The three-parameter power model contains three parameters: initial connection stiffness,  $R_{ki}$ , ultimate connection moment capacity,  $M_u$ , and shape parameter,  $n$ . The power model may be written as (Figure 28.7):

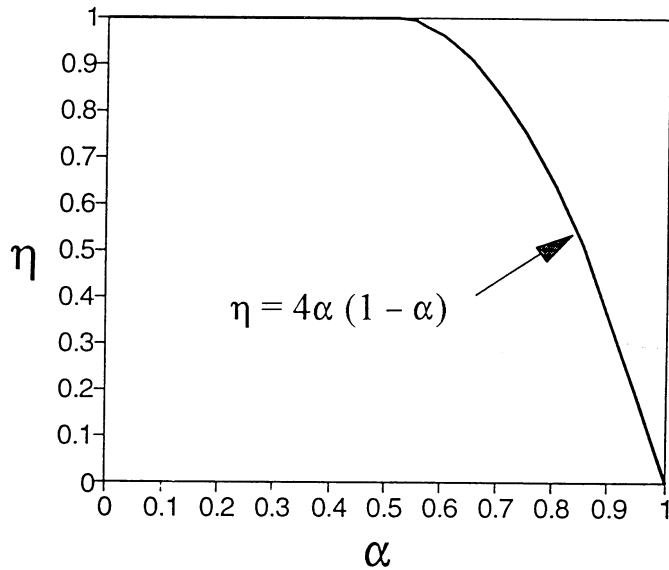


FIGURE 28.5: Parabolic plastic hinge stiffness degradation function with  $\alpha_0 = 0.5$  based on the load and resistance factor design sectional strength equation.

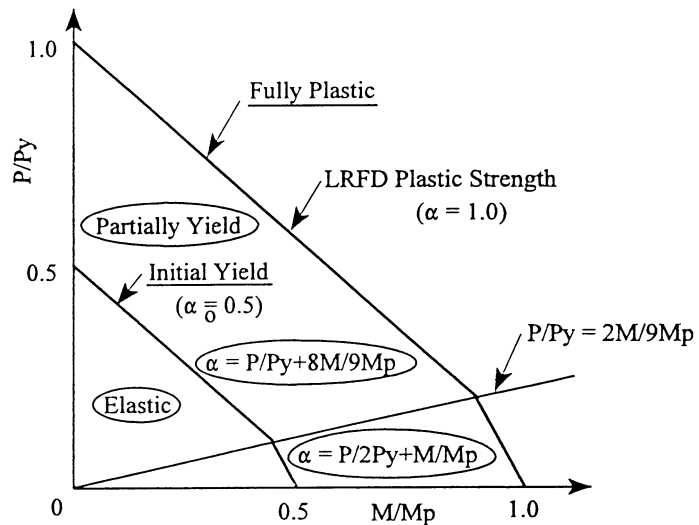


FIGURE 28.6: Smooth stiffness degradation for a work-hardening plastic hinge based on the load and resistance factor design sectional strength curve.

$$m = \frac{\theta}{(1 + \theta^n)^{1/n}} \text{ for } \theta > 0, \quad m > 0 \quad (28.7)$$

where  $m = M/M_u$ ,  $\theta = \theta_r/\theta_o$ ,  $\theta_o$  = reference plastic rotation,  $M_u/R_{ki}$ ,  $M_u$  = ultimate moment capacity of the connection,  $R_{ki}$  = initial connection stiffness, and  $n$  = shape parameter. When the connection is loaded, the connection tangent stiffness,  $R_{kt}$ , at an arbitrary rotation,  $\theta_r$ , can be derived by simply differentiating Equation 28.7 as:

$$R_{kt} = \frac{dM}{d|\theta_r|} = \frac{M_u}{\theta_o (1 + \theta_o^n)^{1+1/n}} \quad (28.8)$$

When the connection is unloaded, the tangent stiffness is equal to the initial stiffness as:

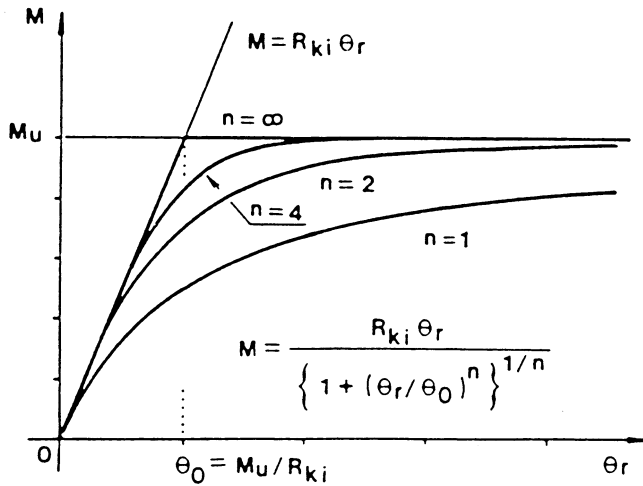


FIGURE 28.7: Moment-rotation behavior of the three-parameter model.

$$R_{kt} = \frac{dM}{d|\theta_r|} = \frac{M_u}{\theta_o} = R_{ki} \quad (28.9)$$

It is observed that a small value of the power index,  $n$ , makes a smooth transition curve from the initial stiffness,  $R_{kt}$ , to the ultimate moment,  $M_u$ . On the contrary, a large value of the index,  $n$ , makes the transition more abruptly. In the extreme case, when  $n$  is infinity, the curve becomes a bilinear line consisting of the initial stiffness,  $R_{ki}$ , and the ultimate moment capacity,  $M_u$ .

#### Practical Estimation of Three Parameters Using Computer Program

An important task for practical use of the power model is to determine the three parameters for a given connection configuration. One difficulty in determining the three parameters is the need for numerical iteration, especially to estimate the ultimate moment,  $M_u$ . A set of nomographs was proposed by Kishi et al. [22] to overcome the difficulty. Even though the purpose of these nomographs is to allow the engineer to rapidly determine the three parameters for a given connection configuration, the nomographs require other efforts for engineers to know how to use them, and the values of the nomographs are approximate.

Herein, one simple way to avoid the difficulties described above is presented. A direct and easy estimation of the three parameters may be achieved by use of a simple computer program 3PARA.f. The operating procedure of the program is shown in Figure 28.8. The input data, CONN.DAT, may be easily generated corresponding to the input format listed in Table 28.2.

As for the shape parameter,  $n$ , the equations developed by Kishi et al. [22] are implemented here. Using a statistical technique for  $n$  values, empirical equations of  $n$  are determined as a linear function of  $\log_{10} \theta_o$ , shown in Table 28.3. This  $n$  value may be calculated using 3PARA.f.

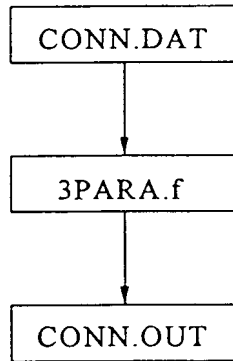


FIGURE 28.8: Operating procedure of computer program estimating the three parameters.

**TABLE 28.2** Input Format

Line	Input data					Remark
1	ITYPE	$F_y$	$E$	Connection type and material properties		
2	$l_t$	$t_t$	$k_t$	$g_t$	W	Top/ seat-angle data
3	$l_a$	$t_a$	$k_a$	$g_a$	d	Web-angle data
ITYPE	=	Connection type (1 = top and seat-angle connection, 2 = with web-angle connection)				
$F_y$	=	yield strength of angle				
$E$	=	Young's modulus ( $= 29,000$ ksi)				
$l_t$	=	length of top angle				
$t_t$	=	thickness of top angle				
$k_t$	=	$k$ value of top angle				
$g_t$	=	gauge of top angle ( $= 2.5$ in., typical)				
$W$	=	width of nut ( $W = 1.25$ in. for $3/4D$ bolt, $W = 1.4375$ in. for $7/8D$ bolt)				
$d$	=	depth of beam				
$l_a$	=	length of web angle				
$t_a$	=	thickness of web angle				
$k_a$	=	$k$ value of web angle				
$g_a$	=	gauge of web angle				

*Note:*

- (1) Top- and seat-angle connections need lines 1 and 2 for input data, and top and seat angle with web-angle connections need lines 1, 2, and 3.
- (2) All input data are in free format.
- (3) Top- and seat-angle sizes are assumed to be the same.
- (4) Bolt sizes of top angle, seat angle, and web angle are assumed to be the same.

**TABLE 28.3** Empirical Equations for Shape Parameter,  $n$

Connection type	$n$
Single web-angle connection	$0.520 \log_{10} \theta_o + 2.291$ 0.695
Double web-angle connection	$1.322 \log_{10} \theta_o + 3.952$ 0.573
Top- and seat-angle connection	$2.003 \log_{10} \theta_o + 6.070$ 0.302
Top- and seat-angle connection with double web angle	$1.398 \log_{10} \theta_o + 4.631$ 0.827

From Kishi, N., Goto, Y., Chen, W. F., and Matsuoka, K. G. 1993. *Eng. J. AISC*, pp. 90-107. With permission.

### Load-Displacement Relationship Accounting for Semi-Rigid Connection

The connection may be modeled as a rotational spring in the moment-rotation relationship represented by Equation 28.10. Figure 28.9 shows a beam-column element with **semi-rigid connections** at both ends. If the effect of connection flexibility is incorporated into the member stiffness, the

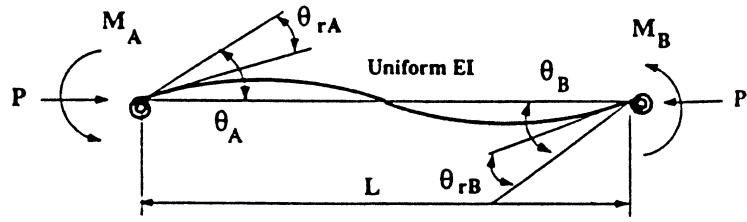


FIGURE 28.9: Beam-column element with semi-rigid connections.

incremental element force-displacement relationship of Equation 28.1 is modified as [24]:

$$\begin{bmatrix} \dot{M}_A \\ \dot{M}_B \\ \dot{P} \end{bmatrix} = \frac{E_t I}{L} \begin{bmatrix} S_{ii}^* & S_{ij}^* & 0 \\ S_{ij}^* & S_{jj}^* & 0 \\ 0 & 0 & A/I \end{bmatrix} \begin{bmatrix} \dot{\theta}_A \\ \dot{\theta}_B \\ \dot{e} \end{bmatrix} \quad (28.10)$$

where

$$S_{ii}^* = \left( S_{ij} + \frac{E_t I S_{ii} S_{jj}}{L R_{ktB}} - \frac{E_t I S_{ij}^2}{L R_{ktB}} \right) / R^* \quad (28.11a)$$

$$S_{jj}^* = \left( S_{jj} + \frac{E_t I S_{ii} S_{jj}}{L R_{ktA}} - \frac{E_t I S_{ij}^2}{L R_{ktA}} \right) / R^* \quad (28.11b)$$

$$S_{ij}^* = S_{ij} / R^* \quad (28.11c)$$

$$R^* = \left( 1 + \frac{E_t I S_{ii}}{L R_{ktA}} \right) \left( 1 + \frac{E_t I S_{jj}}{L R_{ktB}} \right) - \left( \frac{E_t I}{L} \right)^2 \frac{S_{ij}^2}{R_{ktA} R_{ktB}} \quad (28.11d)$$

where  $R_{ktA}$ ,  $R_{ktB}$  = tangent stiffness of connections A and B, respectively;  $S_{ii}$ ,  $S_{ij}$  = generalized stability functions; and  $S_{ii}^*$ ,  $S_{jj}^*$  = modified stability functions that account for the presence of end connections. The tangent stiffness ( $R_{ktA}$ ,  $R_{ktB}$ ) accounts for the different types of semi-rigid connections (see Equation 28.8).

### 28.2.3 Geometric Imperfection Methods

Geometric imperfection modeling combined with the CRC tangent modulus model is discussed in what follows. There are three: the explicit imperfection modeling method, the equivalent notional load method, and the further reduced tangent modulus method.

#### Explicit Imperfection Modeling Method

##### Braced Frame

The refined plastic hinge analysis implicitly accounts for the effects of both residual stresses and spread of yielded zones. To this end, refined plastic hinge analysis may be regarded as equivalent to the plastic-zone analysis. As a result, geometric imperfections are necessary only to consider fabrication error. For braced frames, member out-of-straightness, rather than frame out-of-plumbness, needs to be used for geometric imperfections. This is because the  $P - \Delta$  effect due to the frame out-of-plumbness is diminished by braces. The ECCS [10, 11], AS [30], and Canadian Standard Association (CSA) [4, 5] specifications recommend an initial crookedness of column equal to 1/1000 times the

column length. The AISC code recommends the same maximum fabrication tolerance of  $L_c/1000$  for member out-of-straightness. In this study, a geometric imperfection of  $L_c/1000$  is adopted.

The ECCS [10, 11], AS [30], and CSA [4, 5] specifications recommend the out-of-straightness varying parabolically with a maximum in-plane deflection at the midheight. They do not, however, describe how the parabolic imperfection should be modeled in analysis. Ideally, many elements are needed to model the parabolic out-of-straightness of a beam-column member, but it is not practical. In this study, two elements with a maximum initial deflection at the midheight of a member are found adequate for capturing the imperfection. Figure 28.10 shows the out-of-straightness modeling for a braced beam-column member. It may be observed that the out-of-plumbness is equal to 1/500

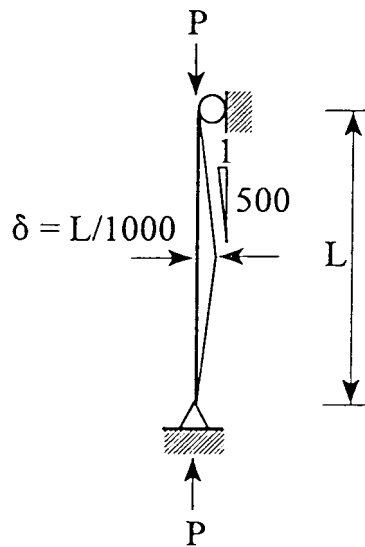


FIGURE 28.10: Explicit imperfection modeling of a braced member.

when the half segment of the member is considered. This value is identical to that of sway frames as discussed in recent papers by Kim and Chen [16, 17, 18]. Thus, it may be stated that the imperfection values are essentially identical for both sway and braced frames. It is noted that this explicit modeling method in braced frames requires the inconvenient imperfection modeling at the center of columns although the inconvenience is much lighter than that of the conventional LRFD method for frame design.

#### Unbraced Frame

The CSA [4, 5] and the AISC codes of standard practice [2] set the limit of erection out-of-plumbness at  $L_c/500$ . The maximum erection tolerances in the AISC are limited to 1 in. toward the exterior of buildings and 2 in. toward the interior of buildings less than 20 stories. Considering the maximum permitted average lean of 1.5 in. in the same direction of a story, the geometric imperfection of  $L_c/500$  can be used for buildings up to six stories with each story approximately 10 ft high. For taller buildings, this imperfection value of  $L_c/500$  is conservative since the accumulated geometric imperfection calculated by 1/500 times building height is greater than the maximum permitted erection tolerance.

In this study, we shall use  $L_c/500$  for the out-of-plumbness without any modification because the system strength is often governed by a weak story that has an out-of-plumbness equal to  $L_c/500$  [27]

and a constant imperfection has the benefit of simplicity in practical design. The explicit geometric imperfection modeling for an unbraced frame is illustrated in Figure 28.11.

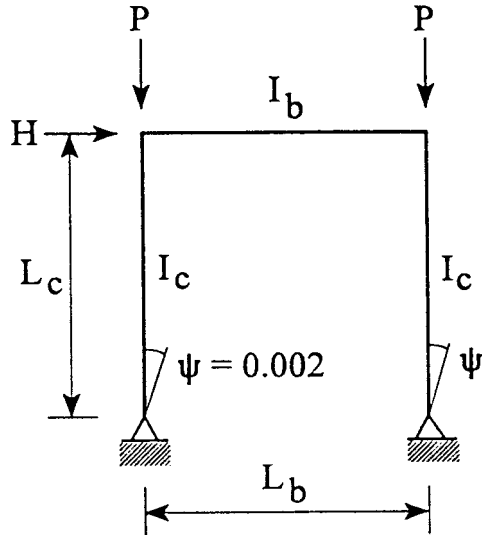


FIGURE 28.11: Explicit imperfection modeling of an unbraced frame.

### Equivalent Notional Load Method

#### Braced Frame

The ECCS [10, 11] and the CSA [4, 5] introduced the equivalent load concept, which accounted for the geometric imperfections in unbraced frames, but not in braced frames. The notional load approach for braced frames is also necessary to use the proposed methods for braced frames.

For braced frames, an equivalent notional load may be applied at midheight of a column since the ends of the column are braced. An equivalent notional load factor equal to 0.004 is proposed here, and it is equivalent to the out-of-straightness of  $L_c/1000$ . When the free body of the column shown in Figure 28.12 is considered, the notional load factor,  $\alpha$ , results in 0.002 with respect to one-half of the member length. Here, as in explicit imperfection modeling, the equivalent notional load factor is the same in concept for both sway and braced frames.

One drawback of this method for braced frames is that it requires tedious input of notional loads at the center of each column. Another is the axial force in the columns must be known in advance to determine the notional loads before analysis, but these are often difficult to calculate for large structures subject to lateral wind loads. To avoid this difficulty, it is recommended that either the explicit imperfection modeling method or the further reduced tangent modulus method be used.

#### Unbraced Frame

The geometric imperfections of a frame may be replaced by the equivalent notional lateral loads expressed as a fraction of the gravity loads acting on the story. Herein, the equivalent notional load factor of 0.002 is used. The notional load should be applied laterally at the top of each story. For sway frames subject to combined gravity and lateral loads, the notional loads should be added to the lateral loads. Figure 28.13 shows an illustration of the equivalent notional load for a portal frame.

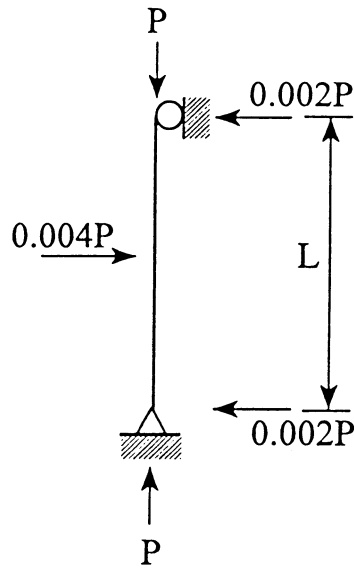


FIGURE 28.12: Equivalent notional load modeling for geometric imperfection of a braced member.

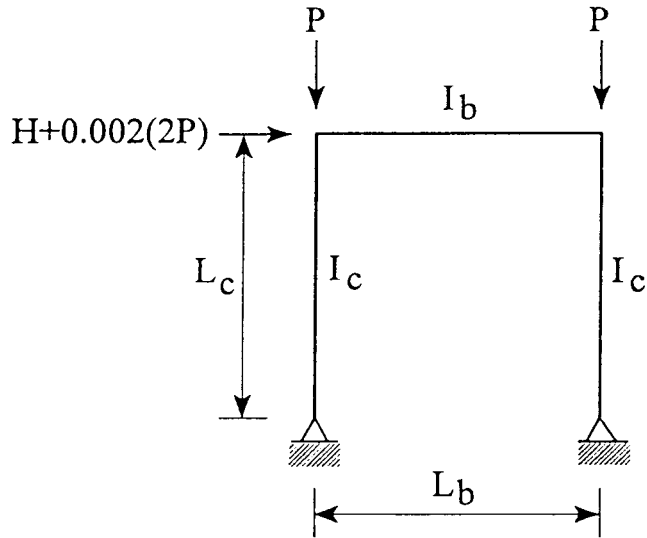


FIGURE 28.13: Equivalent notional load modeling for geometric imperfection of an unbraced frame.

### Further Reduced Tangent Modulus Method

#### Braced Frame

The idea of using the reduced tangent modulus concept is to further reduce the tangent modulus,  $E_t$ , to account for further stiffness degradation due to geometrical imperfections. The degradation of member stiffness due to geometric imperfections may be simulated by an equivalent reduction of member stiffness. This may be achieved by a further reduction of tangent modulus as [15, 16]:

$$E'_t = 4 \frac{P}{P_y} \left( 1 - \frac{P}{P_y} \right) E \xi_i \text{ for } P > 0.5 P_y \quad (28.12a)$$

$$E'_t = E \xi_i \text{ for } P \leq 0.5 P_y \quad (28.12b)$$

where

$E'_t$  = reduced  $E_t$

$\xi_i$  = reduction factor for geometric imperfection

Herein, the reduction factor of 0.85 is used, and the further reduced tangent modulus curves for the CRC  $E_t$  with geometric imperfections are shown in Figure 28.14. The further reduced tangent

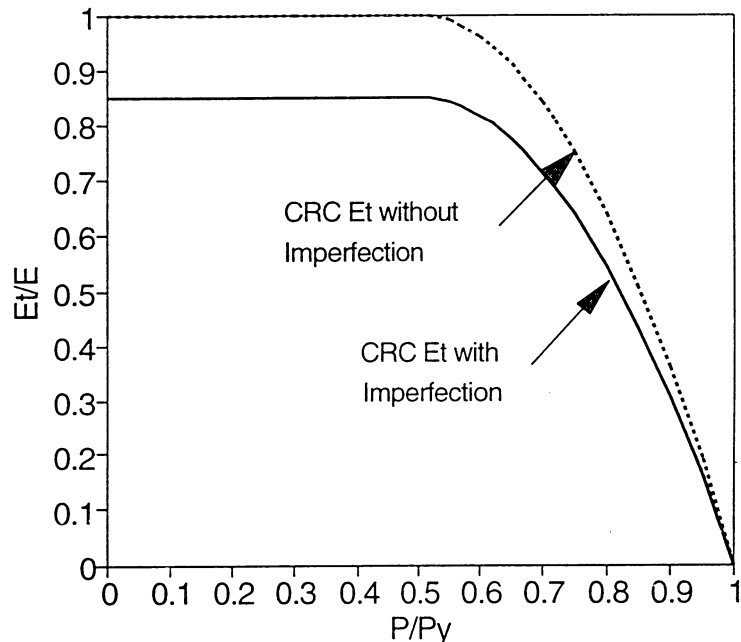


FIGURE 28.14: Further reduced CRC tangent modulus for members with geometric imperfections.

modulus concept satisfies one of the requirements for advanced analysis recommended by the SSRC task force report [29], that is: “The geometric imperfections should be accommodated implicitly within the element model. This would parallel the philosophy behind the development of most modern column strength expressions. That is, the column strength expressions in specifications such as the AISC-LRFD implicitly include the effects of residual stresses and out-of-straightness.”

The advantage of this method over the other two methods is its convenience for design use, because it eliminates the inconvenience of explicit imperfection modeling or equivalent notional loads. Another benefit of this method is that it does not require the determination of the direction of geometric imperfections, often difficult to determine in a large system. On the other hand, in other two methods, the direction of geometric imperfections must be taken correctly in coincidence with the deflection direction caused by bending moments, otherwise the wrong direction of geometric imperfection in braced frames may help the bending stiffness of columns rather than reduce it.

#### Unbraced Frame

The idea of the further reduced tangent modulus concept may also be used in the analysis of unbraced frames. Herein, as in the braced frame case, an appropriate reduction factor of 0.85 to  $E_t$  can be used [18, 19, 20]. The advantage of this approach over the other two methods is its convenience and simplicity because it completely eliminates the inconvenience of explicit imperfection modeling or the notional load input.

#### 28.2.4 Numerical Implementation

The nonlinear global solution methods may be divided into two subgroups: (1) iterative methods and (2) simple incremental method. Iterative methods such as Newton-Raphson, modified Newton-Raphson, and quasi-Newton satisfy equilibrium equations at specific external loads. In these methods, the equilibrium out-of-balance present following the linear load step is eliminated (within tolerance) by taking corrective steps. The iterative methods possess the advantage of providing the exact load-displacement frame; however, they are inefficient, especially for practical purposes, in the trace of the hinge-by-hinge formation due to the requirement of the numerical iteration process.

The simple incremental method is a direct nonlinear solution technique. This numerical procedure is straightforward in concept and implementation. The advantage of this method is its computational efficiency. This is especially true when the structure is loaded into the inelastic region since tracing the hinge-by-hinge formation is required in the element stiffness formulation. For a finite increment size, this approach approximates only the nonlinear structural response, and equilibrium between the external applied loads and the internal element forces is not satisfied. To avoid this, an improved incremental method is used in this program. The applied load increment is automatically reduced to minimize the error when the change in the element stiffness parameter ( $\Delta\eta$ ) exceeds a defined tolerance. To prevent plastic hinges from forming within a constant-stiffness load increment, load step sizes less than or equal to the specified increment magnitude are internally computed so plastic hinges form only after the load increment. Subsequent element stiffness formations account for the stiffness reduction due to the presence of the plastic hinges. For elements partially yielded at their ends, a limit is placed on the magnitude of the increment in the element end forces.

The applied load increment in the above solution procedure may be reduced for any of the following reasons:

1. Formation of new plastic hinge(s) prior to the full application of incremental loads.
2. The increment in the element nodal forces at plastic hinges is excessive.
3. Nonpositive definiteness of the structural stiffness matrix.

As the stability limit point is approached in the analysis, large step increments may overstep a limit point. Therefore, a smaller step size is used near the limit point to obtain accurate collapse displacements and second-order forces.

### 28.3 Verifications

---

In the previous section, a practical advanced analysis method was presented for a direct two-dimensional frame design. The practical approach of geometric imperfections and of semi-rigid connections was also discussed together with the advanced analysis method. The practical advanced analysis method was developed using simple modifications to the conventional elastic-plastic hinge analysis.

In this section, the practical advanced analysis method will be verified by the use of several benchmark problems available in the literature. Verification studies are carried out by comparing with the plastic-zone solutions as well as the conventional LRFD solutions. The strength predictions and

the load-displacement relationships are checked for a wide range of steel frames including axially loaded columns, portal frame, six-story frame, and semi-rigid frames [15]. The three imperfection modelings, including explicit imperfection modeling, equivalent notional load modeling, and further reduced tangent modulus modeling, are also verified for a wide range of steel frames [15]).

### 28.3.1 Axially Loaded Columns

The AISC-LRFD column strength curve is used for the calibration since it properly accounts for second-order effects, residual stresses, and geometric imperfections in a practical manner. In this study, the column strength of proposed methods is evaluated for columns with slenderness parameters,  $[\lambda_c = \frac{KL}{r} \sqrt{F_y/(\pi^2 E)}]$ , varying from 0 to 2, which is equivalent to slenderness ratios ( $L/r$ ) from 0 to 180 when the yield stress is equal to 36 ksi.

In explicit imperfection modeling, the two-element column is assumed to have an initial geometric imperfection equal to  $L_c/1000$  at column midheight. The predicted column strengths are compared with the LRFD curve in Figure 28.15. The errors are found to be less than 5% for slenderness ratios up to 140 (or  $\lambda_c$  up to 1.57). This range includes most columns used in engineering practice.

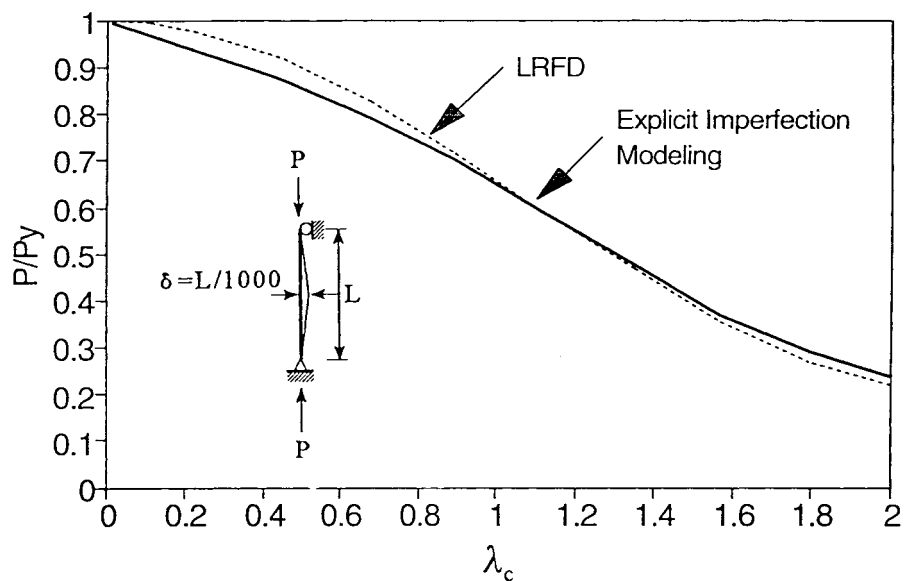


FIGURE 28.15: Comparison of strength curves for an axially loaded pin-ended column (explicit imperfection modeling method).

In the equivalent notional load method, notional loads equal to 0.004 times the gravity loads are applied midheight to the column. The strength predictions are the same as those of the explicit imperfection model (Figure 28.16).

In the further reduced tangent modulus method, the reduced tangent modulus factor equal to 0.85 results in an excellent fit to the LRFD column strengths. The errors are less than 5% for columns of all slenderness ratios. These comparisons are shown in Figure 28.17.

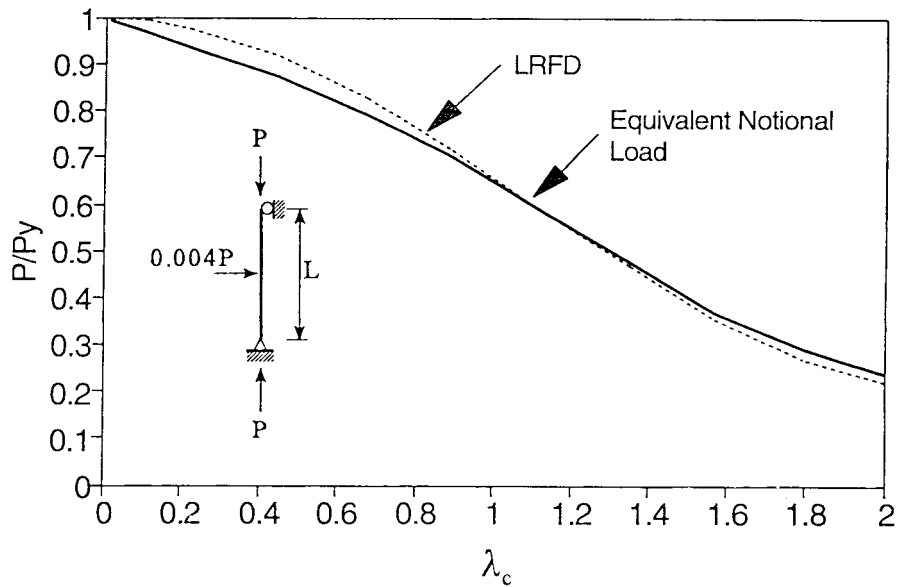


FIGURE 28.16: Comparison of strength curves for an axially loaded pin-ended column (equivalent notional load method).

### 28.3.2 Portal Frame

Kanchanalai [14] performed extensive analyses of portal and leaning column frames, and developed exact interaction curves based on plastic-zone analyses of simple sway frames. Note that the simple frames are more sensitive in their behavior than the highly redundant frames. His studies formed the basis of the interaction equations in the AISC-LRFD design specifications [2, 3]. In his studies, the stress-strain relationship was assumed elastic-perfectly plastic with a 36-ksi yield stress and a 29,000-ksi elastic modulus. The members were assumed to have a maximum compressive residual stress of  $0.3F_y$ . Initial geometric imperfections were not considered, and thus an adjustment of his interaction curves is made to account for this. Kanchanalai further performed experimental work to verify his analyses, which covered a wide range of portal and leaning column frames with slenderness ratios of 20, 30, 40, 50, 60, 70, and 80 and relative stiffness ratios ( $G$ ) of 0, 3, and 4. The ultimate strength of each frame was presented in the form of interaction curves consisting of the nondimensional first-order moment ( $HL_c/2M_p$  in portal frames or  $HL_c/M_p$  in leaning column frames in the  $x$  axis) and the nondimensional axial load ( $P/P_y$  in the  $y$  axis).

In this study, the AISC-LRFD interaction curves are used for strength comparisons. The strength calculations are based on the LeMessurier K factor method [23] since it accounts for story buckling and results in more accurate predictions. The inelastic stiffness reduction factor,  $\tau$  [2], is used to calculate  $K$  in LeMessurier's procedure. The resistance factors  $\phi_b$  and  $\phi_c$  in the LRFD equations are taken as 1.0 to obtain the nominal strength. The interaction curves are obtained by the accumulation of a set of moments and axial forces which result in unity on the value of the interaction equation.

When a geometric imperfection of  $L_c/500$  is used for unbraced frames, including leaning column frames, most of the strength curves fall within an area bounded by the plastic-zone curves and the LRFD curves. In portal frames, the conservative errors are less than 5%, an improvement on the LRFD error of 11%, and the maximum unconservative error is not more than 1%, shown in Figure 28.18. In leaning column frames, the conservative errors are less than 12%, as opposed to the 17% error of the LRFD, and the maximum unconservative error is not more than 5%, as shown in Figure 28.19.

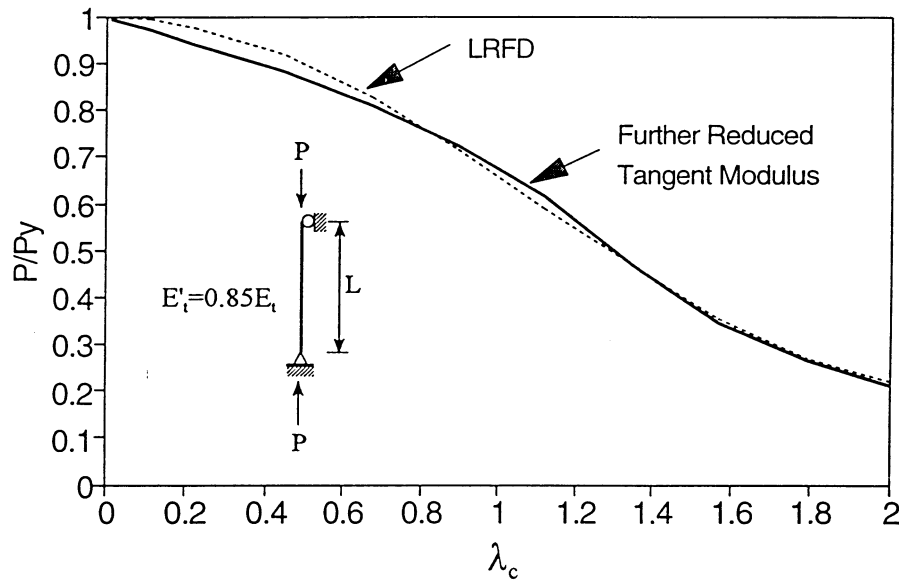


FIGURE 28.17: Comparison of strength curves for an axially loaded pin-ended column (further reduced tangent modulus method).

When a notional load factor of 0.002 is used, the strengths predicted by this method are close to those given by the explicit imperfection modeling method (Figures 28.20 and 28.21).

When the reduced tangent modulus factor of 0.85 is used for portal and leaning column frames, the interaction curves generally fall between the plastic-zone and LRFD curves. In portal frames, the conservative error is less than 8% (better than the 11% error of the LRFD) and the maximum unconservative error is not more than 5% (Figure 28.22). In leaning column frames, the conservative error is less than 7% (better than the 17% error of the LRFD) and the maximum unconservative error is not more than 5% (Figure 28.23).

### 28.3.3 Six-Story Frame

Vogel [32] presented the load-displacement relationships of a six-story frame using plastic-zone analysis. The frame is shown in Figure 28.24. Based on ECCS recommendations, the maximum compressive residual stress is  $0.3F_y$  when the ratio of depth to width ( $d/b$ ) is greater than 1.2, and is  $0.5F_y$  when the  $d/b$  ratio is less than 1.2 (Figure 28.25). The stress-strain relationship is elastic-plastic with strain hardening as shown in Figure 28.26. The geometric imperfections are  $L_c/450$ .

For comparison, the out-of-plumbness of  $L_c/450$  is used in the explicit modeling method. The notional load factor of 1/450 and the reduced tangent modulus factor of 0.85 are used. The further reduced tangent modulus is equivalent to the geometric imperfection of  $L_c/500$ . Thus, the geometric imperfection of  $L_c/4500$  is additionally modeled in the further reduced tangent modulus method, where  $L_c/4500$  is the difference between the Vogel's geometric imperfection of  $L_c/450$  and the proposed geometric imperfection of  $L_c/500$ .

The load-displacement curves for the proposed methods together with the Vogel's plastic-zone analysis are compared in Figure 28.27. The errors in strength prediction by the proposed methods are less than 1%. Explicit imperfection modeling and the equivalent notional load method underpredict lateral displacements by 3%, and the further reduced tangent modulus method shows a

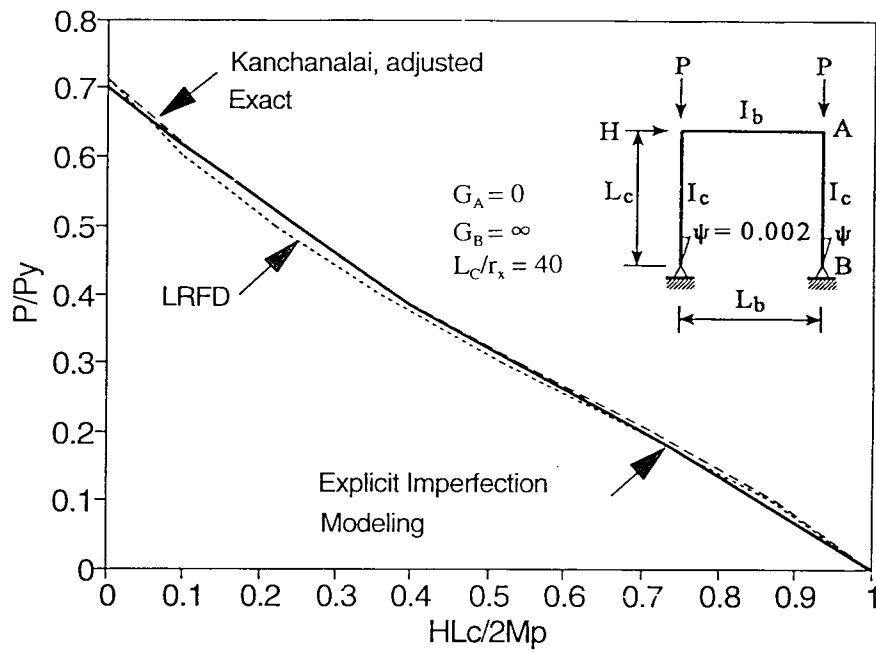


FIGURE 28.18: Comparison of strength curves for a portal frame subject to strong-axis bending with  $L_c/r_x = 40$ ,  $G_A = 0$  (explicit imperfection modeling method).

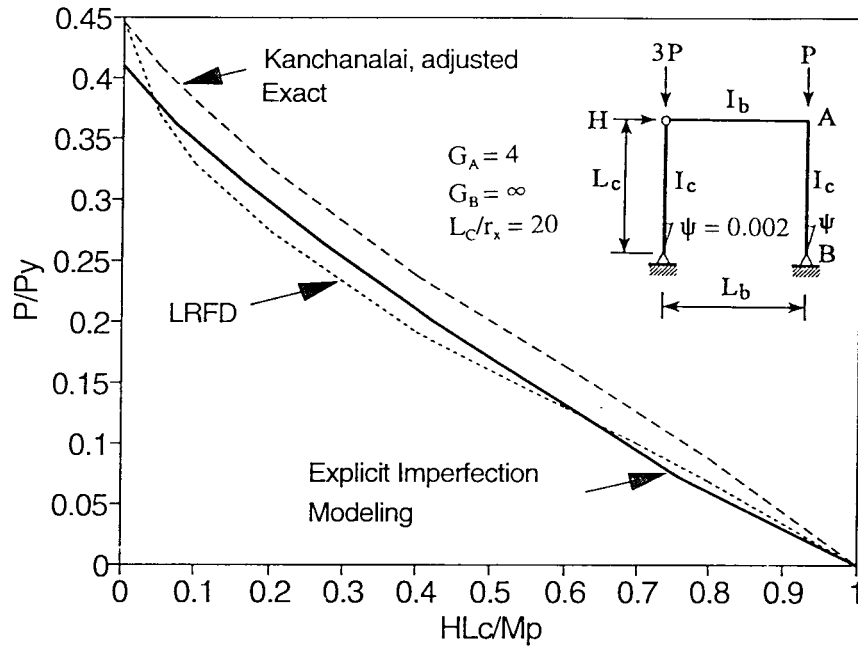


FIGURE 28.19: Comparison of strength curves for a leaning column frame subject to strong-axis bending with  $L_c/r_x = 20$ ,  $G_A = 4$  (explicit imperfection modeling method).

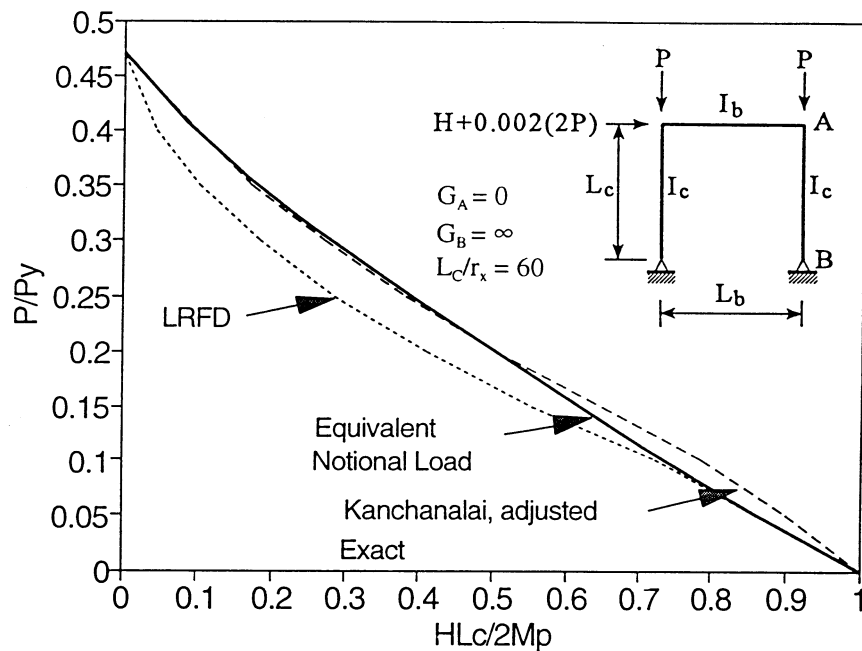


FIGURE 28.20: Comparison of strength curves for a portal frame subject to strong-axis bending with  $L_c/r_x = 60$ ,  $G_A = 0$  (equivalent notional load method).

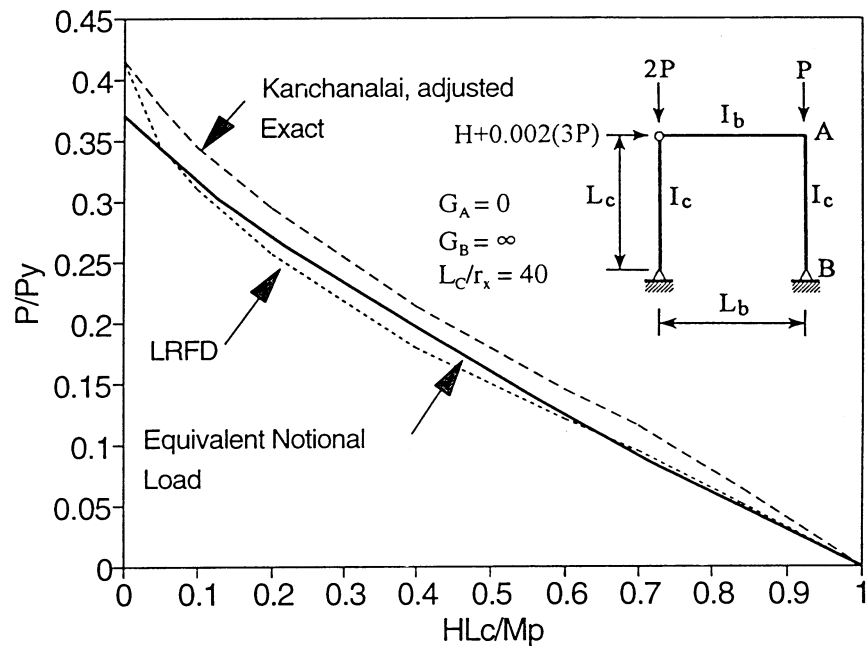


FIGURE 28.21: Comparison of strength curves for a leaning column frame subject to strong-axis bending with  $L_c/r_x = 40$ ,  $G_A = 0$  (equivalent notional load method).

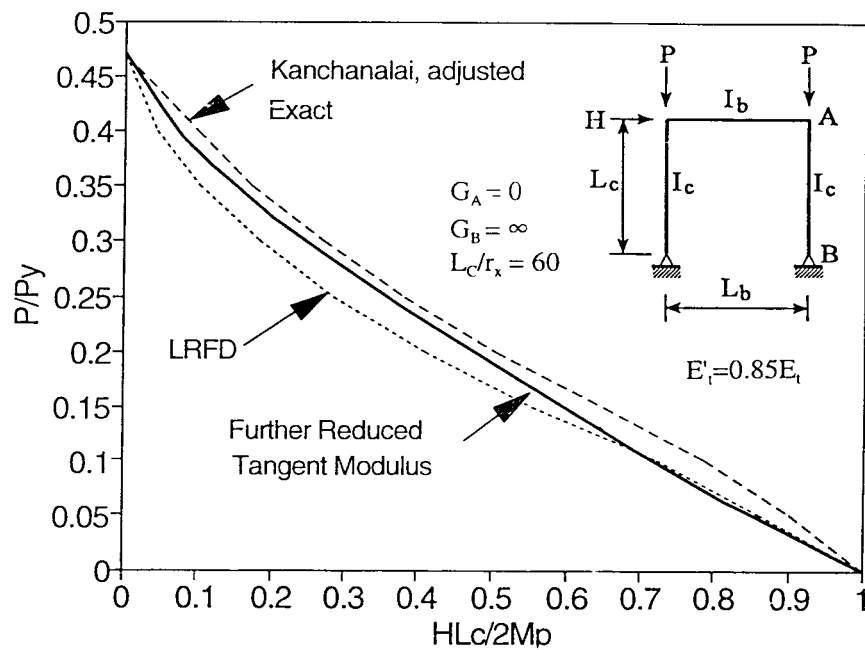


FIGURE 28.22: Comparison of strength curves for a portal frame subject to strong-axis bending with  $L_c/r_x = 60$ ,  $G_A = 0$  (further reduced tangent modulus method).

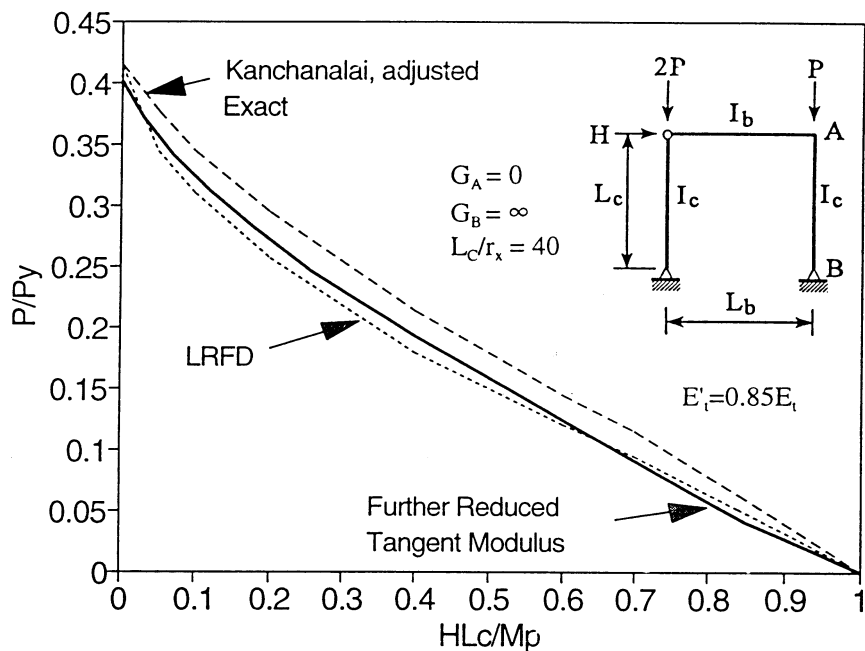


FIGURE 28.23: Comparison of strength curves for a leaning column frame subject to strong-axis bending with  $L_c/r_x = 40$ ,  $G_A = 0$  (further reduced tangent modulus method).

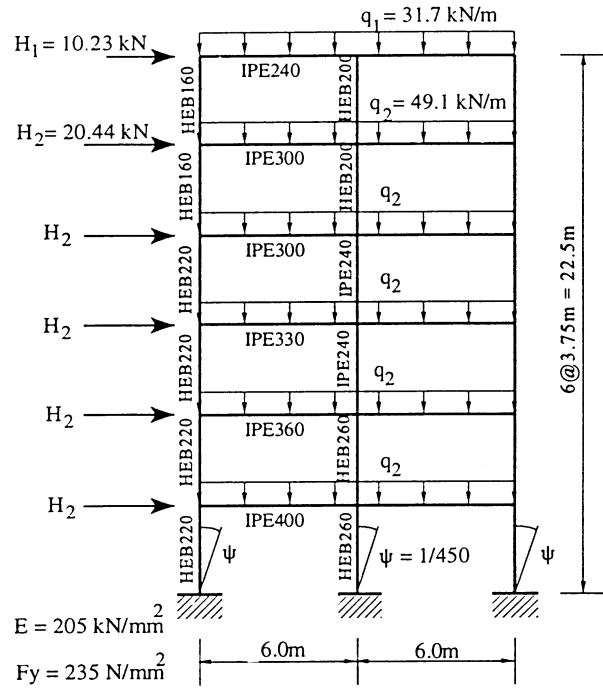


FIGURE 28.24: Configuration and load condition of Vogel's six-story frame for verification study.

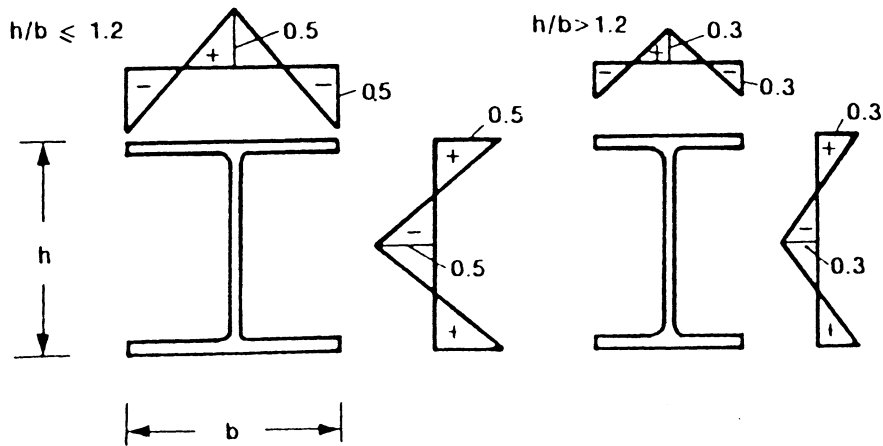
good agreement in displacement with Vogel's exact solution. Vogel's frame is a good example of how the reduced tangent modulus method predicts lateral displacement well under reasonable load combinations.

#### 28.3.4 Semi-Rigid Frame

In the open literature, no benchmark problems solving semi-rigid frames with geometric imperfections are available for a verification study. An alternative is to separate the effects of semi-rigid connections and geometric imperfections. In previous sections, the geometric imperfections were studied and comparisons between proposed methods, plastic-zone analyses, and conventional LRFD methods were made. Herein, the effect of semi-rigid connections will be verified by comparing analytical and experimental results.

Stelmack [31] studied the experimental response of two flexibly connected steel frames. A two-story, one-bay frame in his study is selected as a benchmark for the present study. The frame was fabricated from A36 W5x16 sections, with pinned base supports (Figure 28.28). The connections were bolted top and seat angles (L4x4x1/2) made of A36 steel and A325 3/4-in.-diameter bolts (Figure 28.29). The experimental moment-rotation relationship is shown in Figure 28.30. A gravity load of 2.4 kips was applied at third points along the beam at the first level, followed by a lateral load application. The lateral load-displacement relationship was provided by Stelmack.

Herein, the three parameters of the power model are determined by curve-fitting and the program 3PARA.f is presented in Section 28.2.2. The three parameters obtained by the curve-fit are  $R_{ki} = 40,000$  k-in./rad,  $M_u = 220$  k-in., and  $n = 0.91$ . We obtain three parameters of  $R_{ki} = 29,855$  kips/rad,  $M_u = 185$  k-in. and  $n = 1.646$  with 3PARA.f.



$$\text{Residual stress distributions } \left( \bar{\sigma}_{res} = \frac{\sigma_{res}}{235 \text{N/mm}^2} \right)$$

FIGURE 28.25: Residual stresses of cross-section for Vogel's frame.

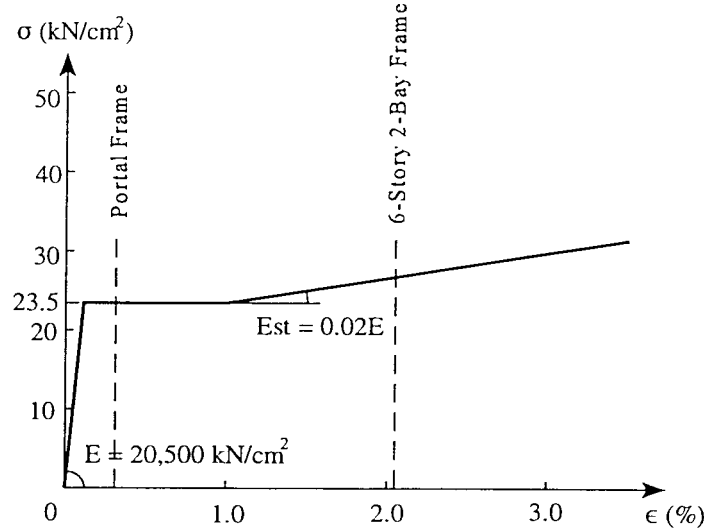


FIGURE 28.26: Stress-strain relationships for Vogel's frame.

The moment-rotation curves given by experiment and curve-fitting show good agreement (Figure 28.30). The parameters given by the Kishi-Chen equations and by experiment show some deviation (Figure 28.30). In spite of this difference, the Kishi-Chen equations, using the computer program (3PARA.f), are a more practical alternative in design since experimental moment-rotation curves are not usually available [19]. In the analysis, the gravity load is first applied, then the lateral load. The lateral displacements given by the proposed methods and by the experimental method

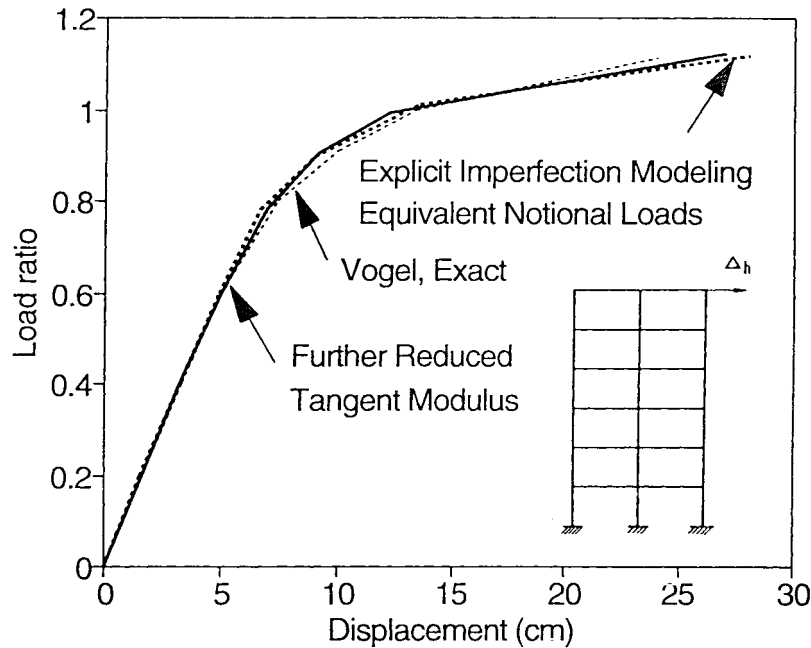


FIGURE 28.27: Comparison of displacements for Vogel's six-story frame.

compare well (Figure 28.31). The proposed method adequately predicts the behavior and strength of semi-rigid connections.

## 28.4 Analysis and Design Principles

In the preceding section, the proposed advanced analysis method was verified using several benchmark problems available in the literature. Verification studies were carried out by comparing it to the plastic-zone and conventional LRFD solutions. It was shown that practical advanced analysis predicted the behavior and failure mode of a structural system with reliable accuracy.

In this section, analysis and design principles are summarized for the practical application of the advanced analysis method. Step-by-step analysis and design procedures for the method are presented.

### 28.4.1 Design Format

Advanced analysis follows the format of LRFD. In LRFD, the factored load effect does not exceed the factored nominal resistance of the structure. Two safety factors are used: one is applied to loads, the other to resistances. This approach is an improvement on other models (e.g., ASD and PD) because both the loads and the resistances have unique factors for unique uncertainties. LRFD has the format

$$\phi R_n \geq \sum_{i=1}^m \gamma_i Q_{ni} \quad (28.13)$$

where

$R_n$  = nominal resistance of the structural member

$Q_n$  = nominal load effect (e.g., axial force, shear force, bending moment)

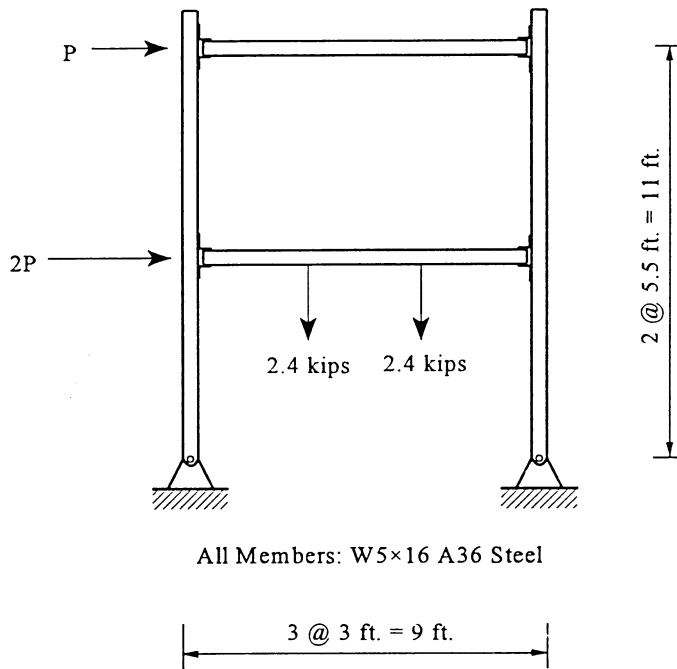


FIGURE 28.28: Configuration and load condition of Stelmack's two-story semi-rigid frame.

- $\phi$  = resistance factor ( $\leq 1.0$ ) (e.g., 0.9 for beams, 0.85 for columns)
- $\gamma_i$  = load factor (usually  $> 1.0$ ) corresponding to  $Q_{ni}$  (e.g., 1.4D and 1.2D + 1.6L + 0.5S)
- $i$  = type of load (e.g., D = dead load, L = live load, S = snow load)
- $m$  = number of load type

Note that the LRFD [2] uses separate factors for each load and therefore reflects the uncertainty of different loads and combinations of loads. As a result, a relatively uniform reliability is achieved.

The main difference between conventional LRFD methods and advanced analysis methods is that the left side of Equation 28.13 ( $\phi R_n$ ) in the LRFD method is the resistance or strength of the component of a structural system, but in the advanced analysis method, it represents the resistance or the load-carrying capacity of the whole structural system.

#### 28.4.2 Loads

Structures are subjected to various loads, including dead, live, impact, snow, rain, wind, and earthquake loads. Structures must be designed to prevent failure and limit excessive deformation; thus, an engineer must anticipate the loads a structure may experience over its service life with reliability.

Loads may be classified as static or dynamic. Dead loads are typical of static loads, and wind or earthquake loads are dynamic. Dynamic loads are usually converted to equivalent static loads in conventional design procedures, and it may be adopted in advanced analysis as well.

#### 28.4.3 Load Combinations

The load combinations in advanced analysis methods are based on the LRFD combinations [2]. Six factored combinations are provided by the LRFD specification. The one must be used to determine member sizes. Probability methods were used to determine the load combinations listed in the LRFD

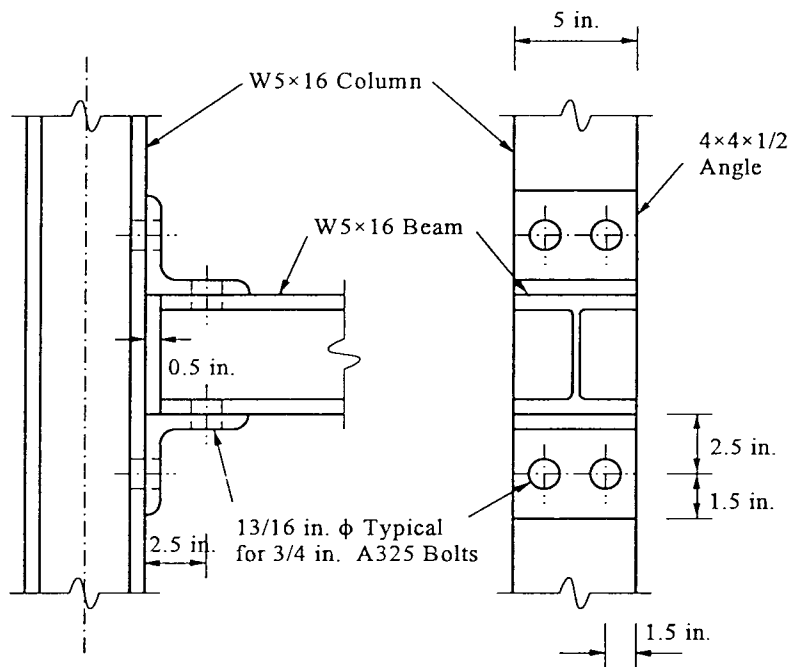


FIGURE 28.29: Top and seat angle connection details.

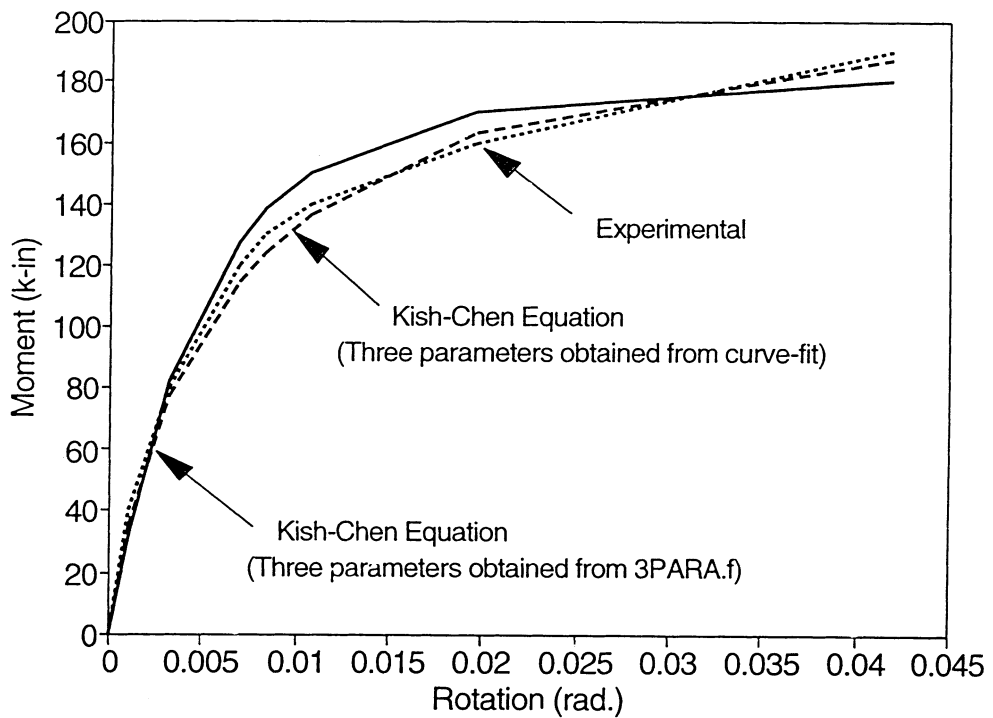


FIGURE 28.30: Comparison of moment-rotation relationships of semi-rigid connection by experiment and the Kishi-Chen equation.

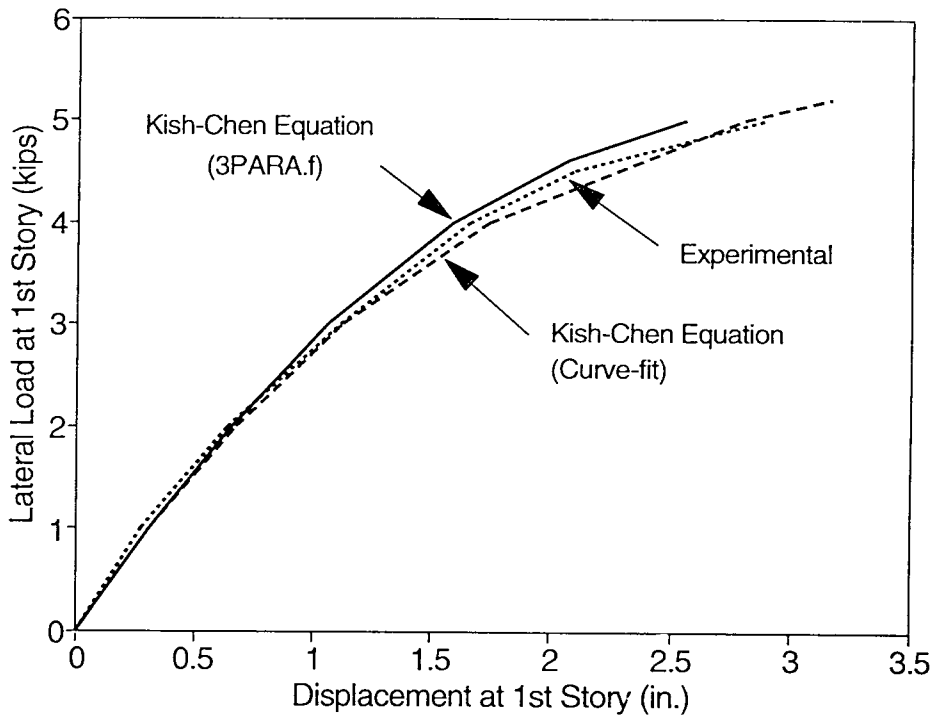


FIGURE 28.31: Comparison of displacements of Stelmack's two-story semi-rigid frame.

specification (LRFD-A4). Each factored load combination is based on the load corresponding to the 50-year recurrence, as follows:

$$(1) 1.4D \quad (28.14a)$$

$$(2) 1.2D + 1.6L + 0.5(L_r \text{ or } S \text{ or } R) \quad (28.14b)$$

$$(3) 1.2D + 1.6(L_r \text{ or } S \text{ or } R) + (0.5L \text{ or } 0.8W) \quad (28.14c)$$

$$(4) 1.2D + 1.3W + 0.5L + 0.5(L_r \text{ or } S \text{ or } R) \quad (28.14d)$$

$$(5) 1.2D \pm 1.0E + 0.5L + 0.2S \quad (28.14e)$$

$$(6) 0.9D \pm (1.3W \text{ or } 1.0E) \quad (28.14f)$$

where

$D$  = dead load (the weight of the structural elements and the permanent features on the structure)

$L$  = live load (occupancy and movable equipment)

$L_r$  = roof live load

$W$  = wind load

$S$  = snow load

$E$  = earthquake load

$R$  = rainwater or ice load.

The LRFD specification specifies an exception that the load factor on live load,  $L$ , in combinations (3)–(5) must be 1.0 for garages, areas designated for public assembly, and all areas where the live load is greater than 100 psf.

#### 28.4.4 Resistance Factors

The AISC-LRFD cross-section strength equations may be written as

$$\frac{P}{\phi_c P_y} + \frac{8M}{9\phi_b M_p} = 1.0 \text{ for } \frac{P}{\phi_c P_y} \geq 0.2 \quad (28.15a)$$

$$\frac{P}{2\phi_c P_y} + \frac{M}{\phi_b M_p} = 1.0 \text{ for } \frac{P}{\phi_c P_y} < 0.2 \quad (28.15b)$$

where

$P, M$  = second-order axial force and bending moment, respectively

$P_y$  = squash load

$M_p$  = plastic moment capacity

$\phi_c, \phi_b$  = resistance factors for axial strength and flexural strength, respectively

Figure 28.32 shows the cross-section strength including the resistance factors,  $\phi_c$  and  $\phi_b$ . The

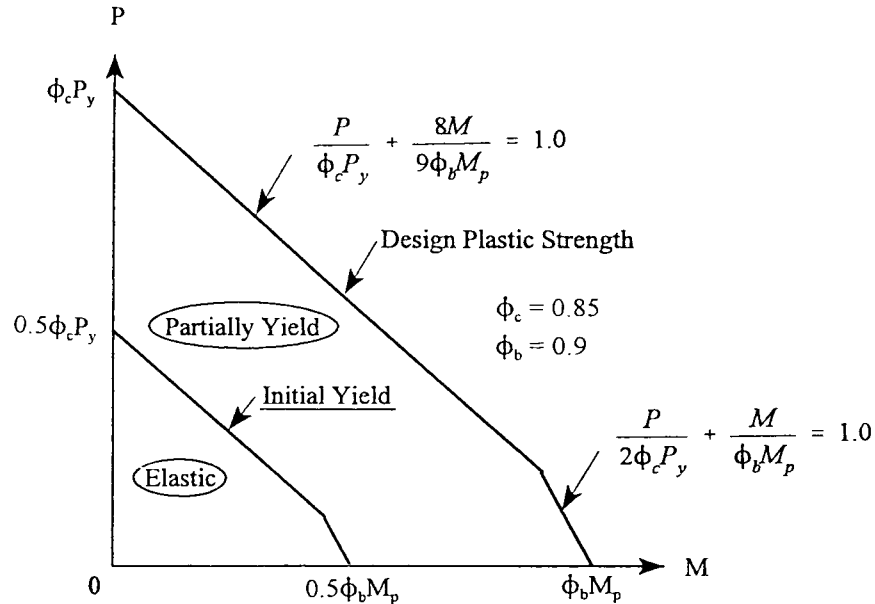


FIGURE 28.32: Stiffness degradation model including reduction factors.

reduction factors,  $\phi_c$  and  $\phi_b$ , are built into the analysis program and are thus automatically included in the calculation of the load-carrying capacity. The reduction factors are 0.85 for axial strength and 0.9 for flexural strength, corresponding to AISC-LRFD specification [2]. For connections, the ultimate moment,  $M_u$ , is reduced by the reduction factor 0.9.

#### 28.4.5 Section Application

The AISC-LRFD specification uses only one column curve for rolled and welded sections of W, WT, and HP shapes, pipe, and structural tubing. The specification also uses some interaction equations for

doubly and singly symmetric members, including W, WT, and HP shapes, pipe, and structural tubing, even though the interaction equations were developed on the basis of W shapes by Kanchanalai [14].

The present advanced analysis method was developed by calibration with the LRFD column curve and interaction equations described in Section 28.3. To this end, it is concluded that the proposed methods can be used for various rolled and welded sections, including W, WT, and HP shapes, pipe, and structural tubing without further modifications.

#### 28.4.6 Modeling of Structural Members

Different types of advanced analysis are (1) plastic-zone method, (2) quasi-plastic hinge method, (3) elastic-plastic hinge method, and (4) refined plastic hinge method. An important consideration in making these advanced analyses practical is the required number of elements for a member in order to predict realistically the behavior of frames.

A sensitivity study of advanced analysis is performed on the required number of elements for a beam member subject to distributed transverse loads. A two-element model adequately predicts the strength of a member. To model parabolic out-of-straightness in a beam-column, a two-element model with a maximum initial deflection at the midheight of a member adequately captures imperfection effects. The required number of elements in modeling each member to provide accurate predictions of the strengths is summarized in Table 28.4. It is concluded that practical advanced analysis is computationally efficient.

**TABLE 28.4** Necessary Number of Elements

Member	Number of elements
Beam member subject to uniform loads	2
Column member of braced frame	2
Column member of unbraced frame	1

#### 28.4.7 Modeling of Geometric Imperfection

Geometric imperfection modeling is required to account for fabrication and erection tolerances. The imperfection modeling methods used here are the explicit imperfection, the equivalent notional load, and the further reduced tangent modulus models. Users may choose one of these three models in an advanced analysis. The magnitude of geometric imperfections is listed in Table 28.5.

**TABLE 28.5** Magnitude of Geometric Imperfection

Geometric imperfection method	Magnitude
Explicit imperfection modeling method	$\psi = 2/1000$ for unbraced frames $\psi = 1/1000$ for braced frames
Equivalent notional load method	$\alpha = 2/1000$ for unbraced frames $\alpha = 4/1000$ for braced frames
Further reduced tangent modulus method	$E'_t = 0.85 E_t$

Geometric imperfection modeling is required for a frame but not a truss element, since the program computes the axial strength of a truss member using the LRFD column strength equations, which account for geometric imperfections.

#### **28.4.8 Load Application**

It is necessary, in an advanced analysis, to input proportional increment load (not the total loads) to trace nonlinear load-displacement behavior. The incremental loading process can be achieved by scaling down the combined factored loads by a number between 10 and 50. For a highly redundant structure (such as one greater than six stories), dividing by about 10 is recommended, and for a nearly statically determinate structure (such as a portal frame), the incremental load may be factored down by 50. One may choose a number between 10 and 50 to reflect the redundancy of a particular structure. Since a highly redundant structure has the potential to form many plastic hinges and the applied load increment is automatically reduced as new plastic hinges form, the larger incremental load (i.e., the smaller scaling number) may be used.

#### **28.4.9 Analysis**

Analysis is important in the proposed design procedures, since the advanced analysis method captures key behaviors including second-order and inelasticity in its analysis program. Advanced analysis does not require separate member capacity checks by the specification equations. On the other hand, the conventional LRFD method accounts for inelastic second-order effects in its design equations (not in analysis). The LRFD method requires tedious separate member capacity checks. Input data used for advanced analysis is easily accessible to users, and the input format is similar to the conventional linear elastic analysis. The format will be described in detail in Section 28.5. Analyses can be simply carried out by executing the program described in Section 28.5. This program continues to analyze with increased loads and stops when a structural system reaches its ultimate state.

#### **28.4.10 Load-Carrying Capacity**

Because consideration at moment redistribution may not always be desirable, the two approaches (including and excluding inelastic moment redistribution) are presented. First, the load-carrying capacity, including the effect of inelastic moment redistribution, is obtained from the final loading step (limit state) given by the computer program. Second, the load-carrying capacity without the inelastic moment redistribution is obtained by extracting that force sustained when the first plastic hinge formed. Generally, advanced analysis predicts the same member size as the LRFD method when moment redistribution is not considered. Further illustrations on these two choices will be presented in Section 28.6.

#### **28.4.11 Serviceability Limits**

The serviceability conditions specified by the LRFD consist of five limit states: (1) deflection, vibration, and [drift](#); (2) thermal expansion and contraction; (3) connection slip; (4) camber; and (5) corrosion. The most common parameter affecting the design serviceability of steel frames is deflection.

Based on the studies by the Ad Hoc Committee [1] and by Ellingwood [12], the deflection limits recommended (Table 28.6) were proposed for general use. At [service load](#) levels, no plastic hinges are permitted anywhere in the structure to avoid permanent deformation under service loads.

#### **28.4.12 Ductility Requirements**

Adequate inelastic rotation capacity is required for members in order to develop their full plastic moment capacity. The required rotation capacity may be achieved when members are adequately braced and their cross-sections are compact. The limitations of compact sections and lateral unbraced

**TABLE 28.6** Deflection Limitations of Frame

Item	Deflection ratio
Floor girder deflection for service live load	$L/360$
Roof girder deflection	$L/240$
Lateral drift for service wind load	$H/400$
Interstory drift for service wind load	$H/300$

length in what follows leads to an inelastic rotation capacity of at least three and seven times the elastic rotation corresponding to the onset of the plastic moment for non-seismic and seismic regions, respectively.

Compact sections are capable of developing the full plastic moment capacity,  $M_p$ , and sustaining large hinge rotation before the onset of local buckling. The compact section in the LRFD specification is defined as:

### 1. Flange

- For non-seismic region

$$\frac{b_f}{2t_f} \leq \frac{65}{\sqrt{F_y}} \quad (28.16)$$

- For seismic region

$$\frac{b_f}{2t_f} \leq \frac{52}{\sqrt{F_y}} \quad (28.17)$$

where

$b_f$  = width of flange  
 $t_f$  = thickness of flange  
 $F_y$  = yield stress in ksi

### 2. Web

- For non-seismic region

$$\frac{h}{t_w} \leq \frac{640}{\sqrt{F_y}} \left(1 - \frac{2.75P_u}{\phi_b P_y}\right) \text{ for } \frac{P}{\phi_b P_y} \leq 0.125 \quad (28.18a)$$

$$\frac{h}{t_w} \leq \frac{191}{\sqrt{F_y}} \left(2.33 - \frac{P_u}{\phi_b P_y}\right) \geq \frac{253}{\sqrt{F_y}} \text{ for } \frac{P}{\phi_b P_y} > 0.125 \quad (28.18b)$$

- For seismic region

$$\frac{h}{t_w} \leq \frac{520}{\sqrt{F_y}} \left(1 - \frac{1.54P_u}{\phi_b P_y}\right) \text{ for } \frac{P}{\phi_b P_y} \leq 0.125 \quad (28.19a)$$

$$\frac{h}{t_w} \leq \frac{191}{\sqrt{F_y}} \left(2.33 - \frac{P_u}{\phi_b P_y}\right) \geq \frac{253}{\sqrt{F_y}} \text{ for } \frac{P}{\phi_b P_y} > 0.125 \quad (28.19b)$$

where

$h$  = clear distance between flanges  
 $t_w$  = thickness of web  
 $F_y$  = yield strength in ksi

In addition to the compactness of section, the lateral unbraced length of beam members is also a limiting factor for the development of the full plastic moment capacity of members. The LRFD provisions provide the limit on spacing of braces for beam as:

- For non-seismic region

$$L_{pd} \leq \frac{[3,600 + 2,200(M_1/M_2)]r_y}{F_y} \quad (28.20a)$$

- For seismic region

$$L_{pd} \leq \frac{2,500r_y}{F_y} \quad (28.20b)$$

where

- $L_{pd}$  = unbraced length
- $r_y$  = radius of gyration about  $y$  axis
- $F_y$  = yield strength in ksi
- $M_1, M_2$  = smaller and larger end moment, respectively
- $M_1/M_2$  = positive in double curvature bending

The AISC-LRFD specification explicitly specifies the limitations for beam members as described above, but not for beam-column members. More studies are necessary to determine the reasonable limits leading to adequate rotation capacity of beam-column members. Based on White's study [33], the limitations for beam members seem to be used for beam-column members until the specification provides the specific values for beam-column members.

#### 28.4.13 Adjustment of Member Sizes

If one of three conditions — strength, serviceability, or **ductility** — is not satisfied, appropriate adjustments of the member sizes should be made. This can be done by referring to the sequence of plastic hinge formation shown in the P . OUT. For example, if the load-carrying capacity of a structural system is less than the factored load effect, the member with the first plastic hinge should be replaced with a stronger member. On the other hand, if the load-carrying capacity exceeds the factored load effect significantly, members without plastic hinges may be replaced with lighter members. If lateral drift exceeds drift requirements, columns or beams should be sized up, or a braced structural system should be considered instead to meet this serviceability limit.

In semi-rigid frames, behavior is influenced by the combined effects of members and connections. As an illustration, if an excessive lateral drift occurs in a structural system, the drift may be reduced by increasing member sizes or using more rigid connections. If the strength of a beam exceeds the required strength, it may be adjusted by reducing the beam size or using more flexible connections. Once the member and connection sizes are adjusted, the iteration leads to an optimum design. Figure 28.33 shows a flow chart of analysis and design procedure in the use of advanced analysis.

## 28.5 Computer Program

---

This section describes the Practical Advanced Analysis Program (PAAP) for two-dimensional steel frame design [15, 24]. The program integrates the methods and techniques developed in Sections 28.2 and 28.3. The names of variables and arrays correspond as closely as possible to those used in

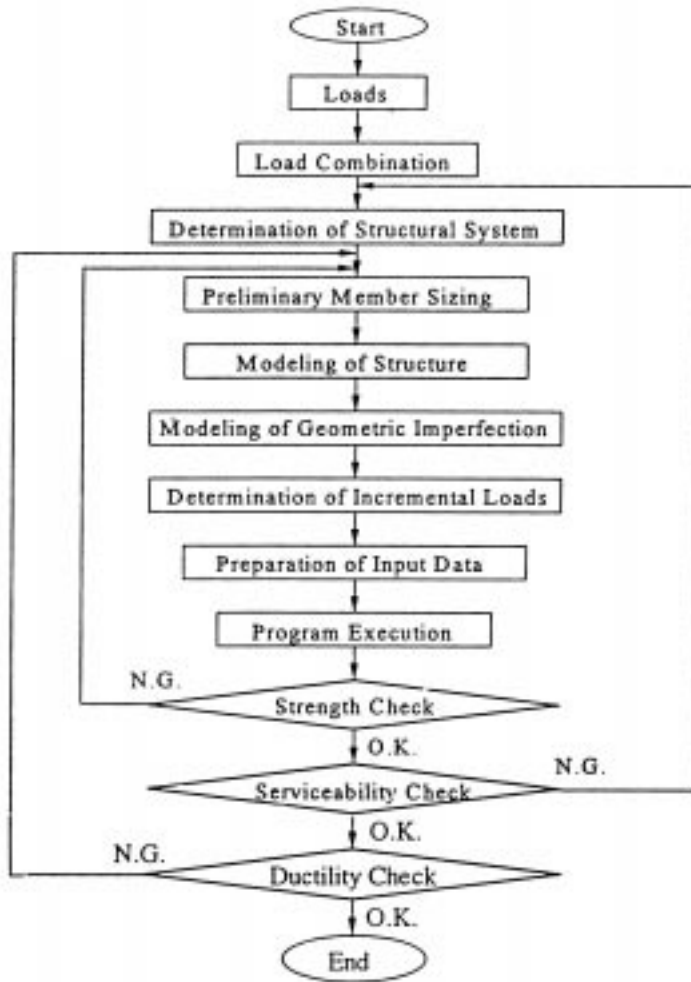


FIGURE 28.33: Analysis and design procedure.

theoretical derivations. The main objective of this section is to present an educational version of software to enable engineers and graduate students to perform planar frame analysis for a more realistic prediction of the strength and behavior of structural systems.

The instructions necessary for user input into PAAP are presented in Section 28.5.4. Except for the requirement to input geometric imperfections and incremental loads, the input data format of the program is basically the same as that of the usual linear elastic analysis program. The user is advised to read all the instructions, paying particular attention to the appended notes, to achieve an overall view of the data required for a specific PAAP analysis. The reader should recognize that no system of units is assumed in the program, and take the responsibility to make all units consistent. Mistaken unit conversion and input are a common source of erroneous results.

### 28.5.1 Program Overview

This FORTRAN program is divided in three: DATAGEN, INPUT, and PAAP. The first program, DATAGEN, reads an input data file, P.DAT, and generates a modified data file, INFIL. The second program, INPUT, rearranges INFIL into three working data files: DATA0, DATA1, and DATA2. The third program, PAAP, reads the working data files and provides two output files named P.OUT1 and P.OUT2. P.OUT1 contains an echo of the information from the input data file, P.DAT. This file may be used to check for numerical and incompatibility errors in input data. P.OUT2 contains the load and displacement information for various joints in the structure as well as the element joint forces for all types of elements at every load step. The load-displacement results are presented at the end of every load increment. The sign conventions for loads and displacements should follow the frame degrees of freedom, as shown in Figures 28.34 and 28.35.

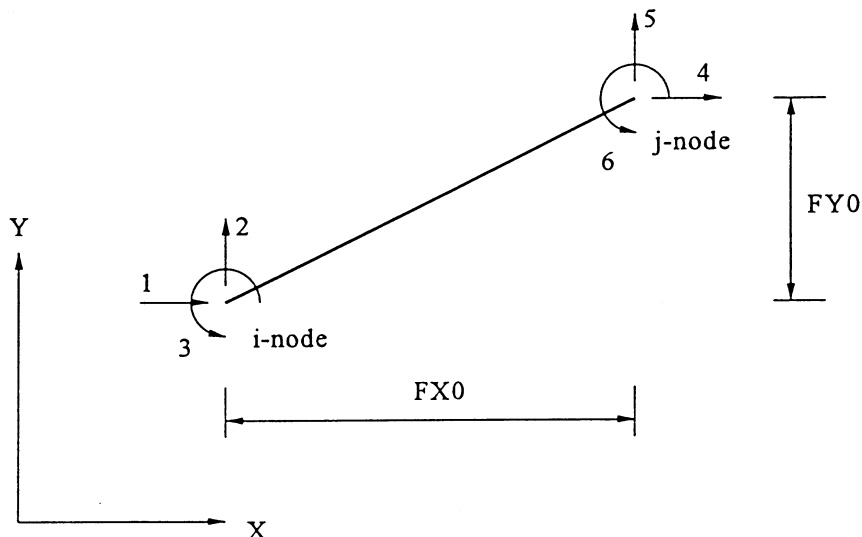


FIGURE 28.34: Degrees of freedom numbering for the frame element.

The element joint forces are obtained by summing the product of the element incremental displacements at every load step. The element joint forces act in the global coordinate system and must be in equilibrium with applied forces. After the output files are generated, the user can view these files on the screen or print them with the MS-DOS PRINT command. The schematic diagram in Figure 28.36 sets out the operation procedure used by PAAP and its supporting programs [15].

### 28.5.2 Hardware Requirements

This program has been tested in two computer processors. First it was tested on an IBM 486 or equivalent personal computer system using Microsoft's FORTRAN 77 compiler v1.00 and Lahey's FORTRAN 77 compiler v5.01. Second, its performance in the workstation environment was tested on a Sun 5 using a Sun FORTRAN 77 compiler. The program sizes of DATAGEN, INPUT, and PAAP are 8 kB, 9 kB, and 94 kB, respectively. The total size of the three programs is small, 111 kB (= 0.111 MB), and so a 3.5-in. high-density diskette (1.44 MB) can accommodate the three programs and several example problems.

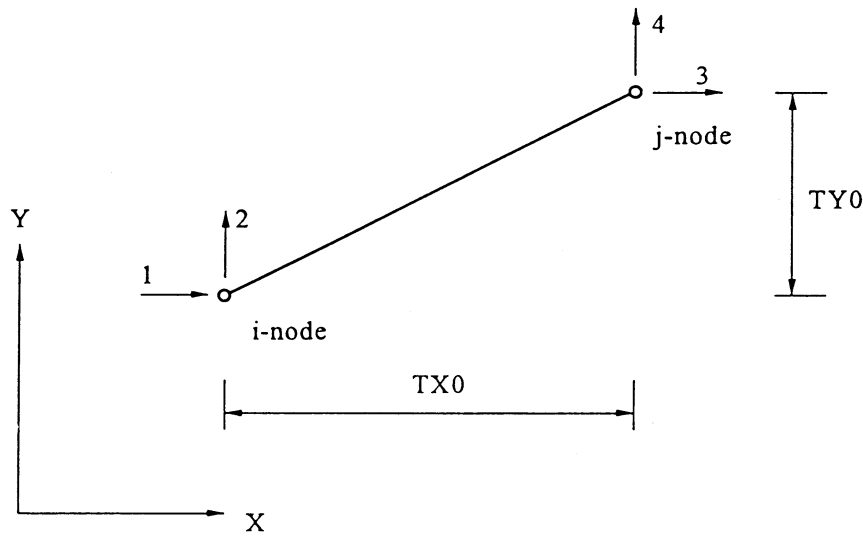


FIGURE 28.35: Degrees of freedom numbering for the truss element.

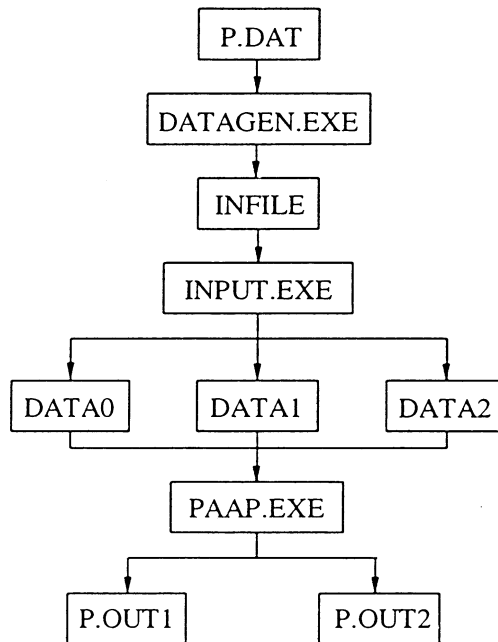


FIGURE 28.36: Operating procedures of the proposed program.

The memory required to run the program depends on the size of the problem. A computer with a minimum 640 K of memory and a 30-MB hard disk is generally required. For the PC applications, the array sizes are restricted as follows:

1. Maximum total degrees of freedom, MAXDOF = 300
2. Maximum translational degrees of freedom, MAXTOF = 300

3. Maximum rotational degrees of freedom, MAXROF = 100
4. Maximum number of truss elements, MAXTRS = 150
5. Maximum number of connections, MAXCNT = 150

It is possible to run bigger jobs in UNIX workstations by modifying the above values in the PARAMETER and COMMON statements in the source code.

### 28.5.3 Execution of Program

A computer diskette is provided in *LRFD Steel Design Using Advanced Analysis*, by W. F. Chen and S. E. Kim, [6], containing four directories with the following files, respectively.

1. Directory PSOURCE
  - DATAGEN.FOR
  - INPUT.FOR
  - PAAP.FOR
2. Directory PTEST
  - DATAGEN.EXE
  - INPUT.EXE
  - PAAP.EXE
  - RUN.BAT (batch file)
  - P.DAT (input data for a test run)
  - P.OUT1 (output for a test run)
  - P.OUT2 (output for a test run)
3. Directory PEXAMPLE
  - All input data for the example problems presented in Section 28.6
4. Directory CONNECT
  - 3PARA.FOR (program for semi-rigid connection parameters)
  - 3PARA.EXE
  - CONN.DAT (input data)
  - CONN.OUT (output for three parameters)

To execute the programs, one must first copy them onto the hard disk (i.e., copy DATAGEN.EXE, INPUT.EXE, PAAP.EXE, RUN.BAT, and P.DAT from the directory PTEST on the diskette to the hard disk). Before launching the program, the user should test the system by running the sample example provided in the directory. The programs are executed by issuing the command RUN. The batch file RUN.BAT executes DATAGEN, INPUT, and PAAP in sequence. The output files produced are P.OUT1 and P.OUT2. When the compilers are different between the authors' and the user's, the program (PAAP.EXE) may not be executed. This problem may be easily solved by recompiling the source programs in the directory PSOURCE.

The input data for all the problems in Section 28.6 are provided in the directory PEXAMPLE. The user may use the input data for his or her reference and confirmation of the results presented in Section 28.6. It should be noted that RUN is a batch command to facilitate the execution of PAAP. Entering the command RUN will write the new files, including DATA0, DATA1, DATA2, P.OUT1,

and P.OUT2, over the old ones. Therefore, output files should be renamed before running a new problem.

The program can generate the output files P.OUT1 and P.OUT2 in a reasonable time period, described in the following. The run time on an IBM 486 PC with memory of 640 K to get the output files for the eight-story frame shown in Figure 28.37 is taken as 4 min 10 s and 2 min 30 s in real time rather than CPU time by using Microsoft FORTRAN and Lahey FORTRAN, respectively. In the Sun 5, the run time varies approximately 2–3 min depending on the degree of occupancy by users.

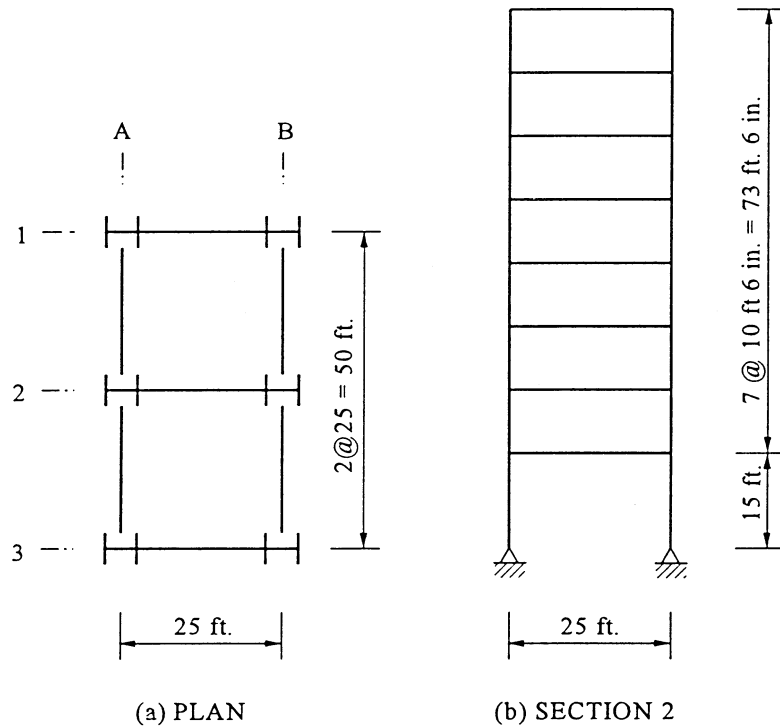


FIGURE 28.37: Configuration of the unbraced eight-story frame.

The directory CONNECT contains the program that computes the three parameters needed for semi-rigid connections. The operation procedure of the program, the input data format, and two examples were presented in Section 28.2.2.

#### 28.5.4 Users' Manual

##### Analysis Options

PAAP was developed on the basis of the theory presented in Section 28.2. While the purpose of the program is basically for advanced analysis using the second-order inelastic concept, the program can be used also for first- and second-order elastic analyses. For a first-order elastic analysis, the total factored load should be applied in one load increment to suppress numerical iteration in the nonlinear analysis algorithm. For a second-order elastic analysis, a yield strength of an arbitrarily large value should be assumed for all members to prevent yielding.

## **Coordinate System**

A two-dimensional ( $x$ ,  $y$ ) global coordinate system is used for the generation of all the input and output data associated with the joints. The following input and output data are prepared with respect to the global coordinate system.

### 1. Input data

- joint coordinates
- joint restraints
- joint load

### 2. Output data

- joint displacement
- member forces

## **Type of Elements**

The analysis library consists of three elements: a plane frame, a plane truss, and a connection. The connection is represented by a zero-length rotational spring element with a user-specified non-linear moment-rotation curve. Loading is allowed only at nodal points. Geometric and material nonlinearities can be accounted for by using an iterative load-increment scheme. Zero-length plastic hinges are lumped at the element ends.

## **Locations of Nodal Points**

The geometric dimensions of the structures are established by placing joints (or nodal points) on the structures. Each joint is given an identification number and is located in a plane associated with a global two-dimensional coordinate system. The structural geometry is completed by connecting the predefined joints with structural elements, which may be a frame, a truss, or a connection. Each element also has an identification number.

The following are some of the factors that need to be considered in placing joints in a structure:

1. The number of joints should be sufficient to describe the initial geometry and the response behavior of the structures.
2. Joints need to be located at points and lines of discontinuity (e.g., at changes in material properties or section properties).
3. Joints should be located at points on the structure where forces and displacements need to be evaluated.
4. Joints should be located at points where concentrated loads will be applied. The applied loads should be concentrated and act on the joints.
5. Joints should be located at all support points. Support conditions are represented in the structural model by restricting the movement of the specific joints in specific directions.
6. Second-order inelastic behavior can be captured by the use of one or two elements per member, corresponding to the following guidelines:
  - Beam member subjected to uniform loads: two elements
  - Column member of braced frame: two elements
  - Column member of unbraced frame: one element

## Degrees of Freedom

A two-joint frame element has six displacement components, as shown in Figure 28.34. Each joint can translate in the global  $x$  and  $y$  directions, and rotate about the global  $z$  axis. The directions associated with these displacement components are known as degrees of freedom of the joint. A two-joint truss element has four degrees of freedom, as shown in Figure 28.35. Each joint has two translational degrees of freedom and no rotational component.

If the displacement of a joint corresponding to any one of its degrees of freedom is known to be zero (such as at a support), then it is labeled an inactive degree of freedom. Degrees of freedom where the displacements are not known are termed active degree of freedoms. In general, the displacement of an inactive degree of freedom is usually known, and the purpose of the analysis is to find the reaction in that direction. For an active degree of freedom, the applied load is known (it could be zero), and the purpose of the analysis is to find the corresponding displacement.

## Units

There are no built-in units in PAAP. The user must prepare the input in a consistent set of units. The output produced by the program will conform to the same set of units. Therefore, if the user chooses to use kips and inches as the input units, all the dimensions of the structure must be entered in inches and all the loads in kips. The material properties should also conform to these units. The output units will then be in kips and inches, so that the frame member axial force will be in kips, bending moments will be in kip-inches, and displacements will be in inches. Joint rotations, however, are in radians, irrespective of units.

## Input Instructions

Described here is the input sequence and data structure used to create an input file called P.DAT. The analysis program, PAAP, can analyze any structure with up to 300 degrees of freedom, but it is possible to recompile the source code to accommodate more degrees of freedom by changing the size of the arrays in the PARAMETER and COMMON statements. The limitation of degrees of freedom can be solved by using dynamic storage allocation. This procedure is common in finite element programs [13, 9], and it will be used in the next release of the program.

The input data file is prepared in a specific format. The input data consists of 13 data sets, including five control data, three section property data, three element data, one boundary condition, and one load data set as follows:

1. Title
2. Analysis and design control
3. Job control
4. Total number of element types
5. Total number of elements
6. Connection properties
7. Frame element properties
8. Truss element properties
9. Connection element data
10. Frame element data
11. Truss element data
12. Boundary conditions
13. Incremental loads

Input of all data sets is mandatory, but some of the data associated with elements (data sets 6–11)

may be skipped, depending on the use of the element. The order of data sets in the input file must be strictly maintained. Instructions for inputting data are summarized in Table 28.7

## 28.6 Design Examples

In previous sections, the concept, verifications, and computer program of the practical advanced analysis method for steel frame design have been presented. The present advanced analysis method has been developed and refined to achieve both simplicity in use and, as far as possible, a realistic representation of behavior and strength. The advanced analysis method captures the limit state strength and stability of a structural system and its individual members. As a result, the method can be used for practical frame design without the tedious separate member capacity checks, including the calculation of K factor.

The aim of this section is to provide further confirmation of the validity of the LRFD-based advanced analysis methods for practical frame design. The comparative design examples in this section show the detailed design procedure for advanced and LRFD design procedures [15]. The design procedures conform to those described in Section 28.4 and may be grouped into four basic steps: (1) load condition, (2) structural modeling, (3) analysis, and (4) limit state check. The design examples cover simple structures, truss structures, braced frames, unbraced frames, and semi-rigid frames. The three practical models — explicit imperfection, equivalent notional load, and further reduced tangent modulus — are used for the design examples. Member sizes determined by advanced procedures are compared with those determined by the LRFD, and good agreement is generally observed.

The design examples are limited to two-dimensional steel frames, so that the spatial behavior is not considered. Lateral torsional buckling is assumed to be prevented by adequate lateral braces. Compact W sections are assumed so that sections can develop their full plastic moment capacity without buckling locally. All loads are statically applied.

### 28.6.1 Roof Truss

Figure 28.38 shows a hinged-jointed roof truss subject to gravity loads of 20 kips at the joints. A36 steel pipe is used. All member sizes are assumed identical.

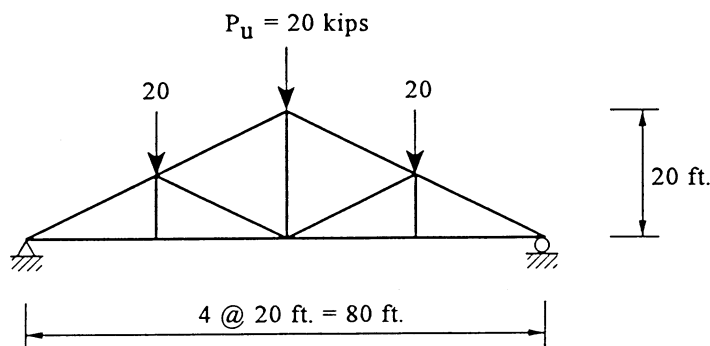


FIGURE 28.38: Configuration and load condition of the hinged-jointed roof truss.

**TABLE 28.7** Input Data Format for the Program PAAP

Data set	Column	Variable	Description
Title	A70	—	Job title and general comments
Analysis and design control	1-5	IGEOIM	Geometric imperfection method 0: No geometric imperfection (default) 1: Explicit imperfection modeling 2: Equivalent notional load 3: Further reduced tangent modulus
	6-10	ILRFD	Strength reduction factor, $\phi_c = 0.85$ , $\phi_b = 0.9$ 0: No reduction factors considered (default) 1: Reduction factors considered
Job control	1-5	NNODE	Total number of nodal points of the structure
	6-10	NBOUND	Total number of supports
	11-15	NINCRE	Allowable number of load increments (default = 100); at least two or three times larger than the scaling number
Total number of element types	1-5	NCTYPE	Number of connection types (1-30)
	6-10	NFTYPE	Number of frame types (1-30)
	11-15	NTTYPE	Number of truss types (1-30)
Total number of elements	1-5	NUMCNT	Number of connection elements (1-150)
	6-10	NUMFRM	Number of frame elements (1-100)
	11-15	NUMTRS	Number of truss elements (1-150)
Connection properties	1-5	ICTYPE	Connection type number
	6-15*	$M_u$	Ultimate moment capacity of connection
	16-25*	$R_{ki}$	Initial stiffness of connection
	26-35*	N	Shape parameter of connection
Frame element properties	1-5	IFTYPE	Frame type number
	6-15*	A	Cross-section area
	6-25*	I	Moment of inertia
	26-35*	Z	Plastic section modulus
	36-45*	E	Modulus of elasticity
	46-55*	FY	Yield stress
	55-60	IFCOL	Identification of column member, IFCOL = 1 for column (default = 0)
Truss element properties	1-5	ITYPE	Truss type number
	6-15*	A	Cross-section area
	16-25*	I	Moment of inertia
	26-35*	E	Modulus of elasticity
	36-45*	FY	Yield stress
	46-50	ITCOL	Identification of column member, ITCOL = 1 for column (default = 0)
Connection element data	1-5	LCNT	Connection element number
	6-10	IFMCNT	Frame element number containing the connection
	11-15	IEND	Identification of element ends containing the connection 1: Connection attached at element end <i>i</i> 2: Connection attached at element end <i>j</i>
	16-20	JDCNT	Connection type number
	21-25	NOSMCN	Number of same elements for automatic generation (default = 1)
	26-30	NELINC	Element number (IFMCNT) increment of automatically generated elements (default = 1)
Frame element data	1-5	LFRM	Frame element number
	6-15*	FXO	Horizontal projected length: positive for <i>i-j</i> direction in global <i>x</i> direction
	16-25*	FYO	Vertical projected length: positive for <i>i-j</i> direction in global <i>y</i> direction
	26-30	JDFRM	Frame type number
	31-35	IFNODE	Number of node <i>i</i>
	36-40	JFNODE	Number of node <i>j</i>
	41-45	NOSMFE	Number of same elements for automatic generation (default = 1)
	46-50	NODINC	Node number increment of automatically generated elements (default = 1)

**TABLE 28.7** Input Data Format for the Program PAAP (*continued*)

Data set	Column	Variable	Description
Truss element data	1-5	LTRS	Truss element number
	6-15*	TXO	Horizontal projected length; positive for $i-j$ direction in global $x$ direction
	16-25*	TYO	Vertical projected length; positive for $i-j$ direction in global $y$ direction
	26-30	JDTRS	Truss type number
	31-35	ITNODE	Number of node $i$
	36-40	JTNODE	Number of node $j$
	51-55	NOSMTE	Number of same elements for automatic generation (default = 1)
	56-60	NODINC	Node number increment of automatically generated elements (default = 1)
	1-5	NODE	Node number of support
	6-10	XFIX	XFIX = 1 for restrained in global $x$ direction (default = 0)
Boundary conditions	11-15	YFIX	YFIX = 1 for restrained in global $y$ direction (default = 0)
	16-20	RFIX	RFIX = 1 for restrained in rotation (default = 0)
	21-25	NOSMBD	Number of same boundary condition for automatic generation (default = 1)
	26-30	NODINC	Node number increment of automatically generated supports (default = 1)
	1-5	NODE	Node number where a load applied
	6-15*	XLOAD	Incremental load in global $x$ direction (default = 0)
	16-25*	YLOAD	Incremental load in global $y$ direction (default = 0)
	26-35*	RLOAD	Incremental moment in global $\theta$ direction (default = 0)
	36-40	NOSMLD	Number of same loads for automatic generation (default = 1)
	41-45	NODINC	Node number increment of automatically generated loads (default = 1)

\* indicates that the real value (F or E format) should be entered; otherwise input the integer value (I format).

## Design by Advanced Analysis

### Step 1: Load Condition and Preliminary Member Sizing

The critical factored load condition is shown in Figure 28.38. The member forces of the truss may be obtained (Figure 28.39) using equilibrium conditions. The maximum compressive force is 67.1 kips. The effective length is the same as the actual length (22.4 ft) since  $K$  is 1.0. The preliminary member size of steel pipe is 6 in. in diameter with 0.28 in. thickness ( $\phi P_n = 81$  kips), obtained using the column design table in the LRFD specification.

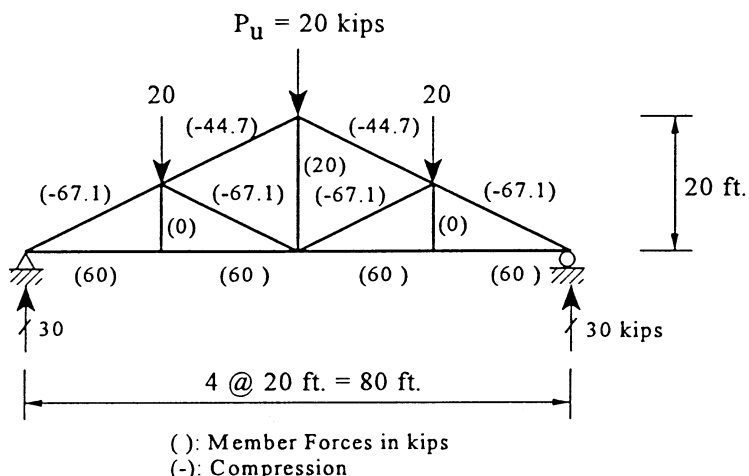


FIGURE 28.39: Member forces of the hinged-jointed roof truss.

### Step 2: Structural Modeling

Each member is modeled with one truss element without geometric imperfection since the program computes the axial strength of the truss member with the LRFD column strength equations, which indirectly account for geometric imperfections. An incremental load of 0.5 kips is determined by dividing the factored load of 20 kips by a scaling factor of 40, as shown in Figure 28.40.

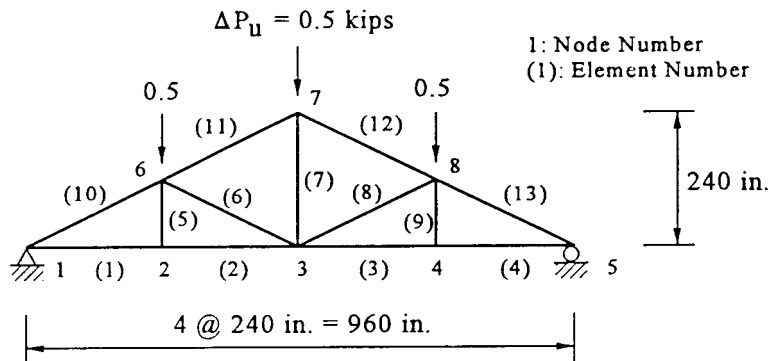


FIGURE 28.40: Modeling of the hinged-jointed roof truss.

### Step 3: Analysis

Referring to the input instructions described in Section 28.5.4, the input data may be easily generated, as listed in Table 28.8. Note that the total number of supports (NBOUND) in the hinged-jointed truss must be equal to the total number of nodal points, since the nodes of a truss element are restrained against rotation. Programs DATAGEN, INPUT, and PAAP are executed in sequence by entering the batch file command RUN on the screen.

### Step 4: Check of Load-Carrying Capacity

Truss elements 10 and 13 fail at load step 48, with loads at nodes 6, 7, and 8 being 24 kips. Since this truss is statically determinant, failure of one member leads to failure of the whole system. Load step 49 shows a sharp increase in displacement and indicates a system failure. The member force of element 10 is 80.4 kips ( $F_x = 72.0$  kips,  $F_y = 35.7$  kips). Since the load-carrying capacity of 24 kips at nodes 6, 7, and 8 is greater than the applied load of 20 kips, the member size is adequate.

### Step 5: Check of Serviceability

Referring to P. OUT2, the deflection at node 3 corresponding to load step 1 is equal to 0.02 in. This deflection may be considered elastic since the behavior of the beam is linear and elastic under small loads. The total deflection of 0.8 in. is obtained by multiplying the deflection of 0.02 in. by the scaling factor of 40. The deflection ratio over the span length is 1/1200, which meets the limitation 1/360. The deflection at the service load will be smaller than that above since the factored load is used for the calculation of deflection above.

### Comparison of Results

The advanced analysis and LRFD methods predict the same member size of steel pipe with 6 in. diameter and 0.28 in. thickness. The load-carrying capacities of element 10 predicted by these two methods are the same, 80.5 kips. This is because the truss system is statically determinant, rendering inelastic moment redistribution of little or no benefit.

**TABLE 28.8** Input Data, P.DAT, of the Hinged-Jointed Roof Truss

Roof truss						
0	1					
8	8	100				
0	0	1				
0	0	13				
1	5.58	28.1	29000.0		36.0	
1	240.0	0.0	1	1	2	4
5	0.0	120.0	1	2	6	
6	-240.0	120.0	2	3	6	
7	0.0	240.0	1	3	7	
8	240.0	120.0	2	3	8	
9	0.0	120.0	1	4	8	
10	240.0	120.0	2	1	6	
11	240.0	120.0	2	6	7	
12	240.0	-120.0	2	7	8	
13	240.0	-120.0	2	8	5	
1	1	1	1			
2			1	3		
5		1	1			
6			1	3		
6				-0.5		3

## 28.6.2 Unbraced Eight-Story Frame

Figure 28.37 shows an unbraced eight-story one-bay frame with hinged supports. All beams are rigidly connected to the columns. The column and beam sizes are the same. All beams are continuously braced about their weak axis. Bending is primarily about the strong axis at the column. A36 steel is used for all members.

### Design by Advanced Analysis

#### Step 1: Load Condition and Preliminary Member Sizing

The uniform gravity loads are converted to equivalent concentrated loads in Figure 28.41. The preliminary column and beam sizes are selected as W33x130 and W21x50.

#### Step 2: Structural Modeling

Each column is modeled with one element since the frame is unbraced and the maximum moment in the member occurs at the ends. Each beam is modeled with two elements.

The explicit imperfection and the further reduced tangent modulus models are used in this example, since they are easier in preparing the input data than equivalent notional load models. Figure 28.42 shows the model for the eight-story frame. The explicit imperfection model uses an out-of-plumbness of 0.2%, and in the further reduced tangent modulus model,  $0.85 E_t$  is used.

Herein, a scaling factor of 10 is used due to the high indeterminacy. The load increment is automatically reduced if the element stiffness parameter,  $\eta$ , exceeds the predefined value 0.1. The 54 load steps required to converge on the solution are given in P.OUT2.

#### Step 3: Analysis

The input data may be easily generated, as listed in Table 28.9a and 28.9b. Programs are executed in sequence by typing the batch file command RUN.

#### Step 4: Check of Load-Carrying Capacity

From the output file, P.OUT, the ultimate load-carrying capacity of the structure is obtained as 5.24 and 5.18 kips with respect to the lateral load at roof in load combination 2 by the imperfection

**Table 28.9a** Input Data, P.DAT, of the Explicit Imperfection Modeling for the Unbraced Eight-Story Frame

Unbraced eight-story frame, explicit imperfection modeling						
1	1					
26	2					
0	2	0				
0	32	0				
1	38.30	6710.00	467.00	29000.00	36.00	
2	14.70	984.00	110.00	29000.00	36.00	
1	0.252	126.00	1 2	1 7		
8	0.360	180.00	1 9	8		
9	0.252	126.00	1 19	18 7		
16	0.360	180.00	1 26	25		
17	150.00	0.00	2 1	10 8		
25	150.00	0.00	2 10	18 8		
9	1 1					
26	1 1					
1	0.512	-1.080				
2	1.020	-1.255		6		
8	1.240	-1.255				
10		-2.160				
11		-2.510		7		
18		-1.080				
19		-1.255		7		

**Table 28.9b** Input Data, P.DAT, of the Explicit Imperfection Modeling for the Unbraced Eight-Story Frame

Unbraced eight-story frame, further reduced tangent modulus						
3	1					
26	2					
0	2	0				
0	32	0				
1	38.30	6710.00	467.00	29000.00	36.00	1
2	14.70	984.00	110.00	29000.00	36.00	
1	0.	126.00	1 2	1 7		
8	0.	180.00	1 9	8		
9	0.	126.00	1 19	18 7		
16	0.	180.00	1 26	25		
17	150.00	0.00	2 1	10 8		
25	150.00	0.00	2 10	18 8		
9	1 1					
26	1 1					
1	0.512	-1.080				
2	1.020	-1.255		6		
8	1.240	-1.255				
10		-2.160				
11		-2.510		7		
18		-1.080				
19		-1.255		7		

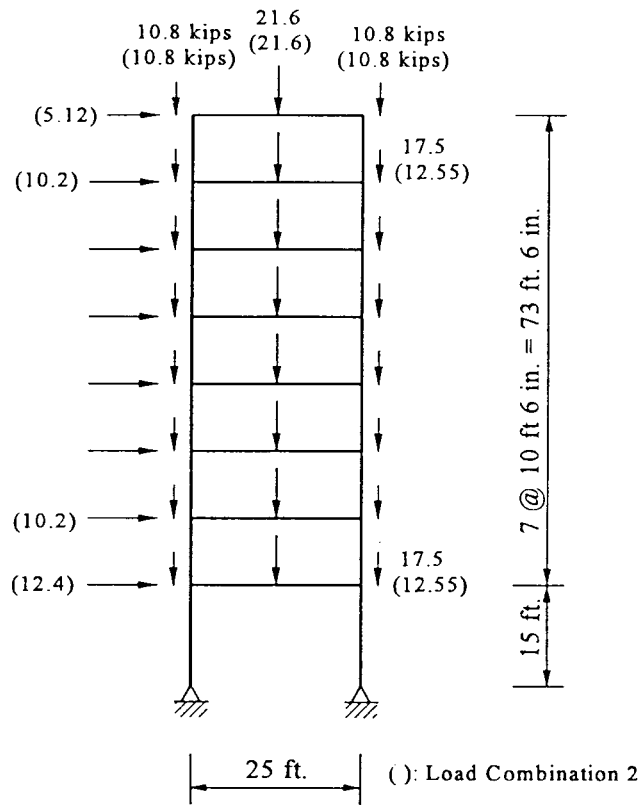


FIGURE 28.41: Concentrated load condition converted from the distributed load for the two-story frame.

method and the reduced tangent modulus method, respectively. This load-carrying capacity is 3 and 2% greater, respectively, than the applied factored load of 5.12 kips. As a result, the preliminary member sizes are satisfactory.

#### Step 5: Check of Serviceability

The lateral drift at the roof level by the wind load ( $1.0W$ ) is 5.37 in. and the drift ratio is 1/198, which does not satisfy the drift limit of 1/400. When W40x174 and W24x76 are used for column and beam members, the lateral drift is reduced to 2.64 in. and the drift ratio is 1/402, which satisfies the limit 1/400. The design of this frame is thus governed by serviceability rather than strength.

#### Comparison of Results

The sizes predicted by the proposed methods are W33x130 columns and W21x50 beams. They do not, however, meet serviceability conditions and must therefore be increased to W40x174 and W24x76 members. The LRFD method results in the same (W40x174) column but a larger (W27x84) beam (Figure 28.43).

### 28.6.3 Two-Story Four-Bay Semi-Rigid Frame

Figure 28.44 shows a two-story four-bay semi-rigid frame. The height of each story is 12 ft and it is 25 ft wide. The spacing of the frames is 25 ft. The frame is subjected to a distributed gravity and

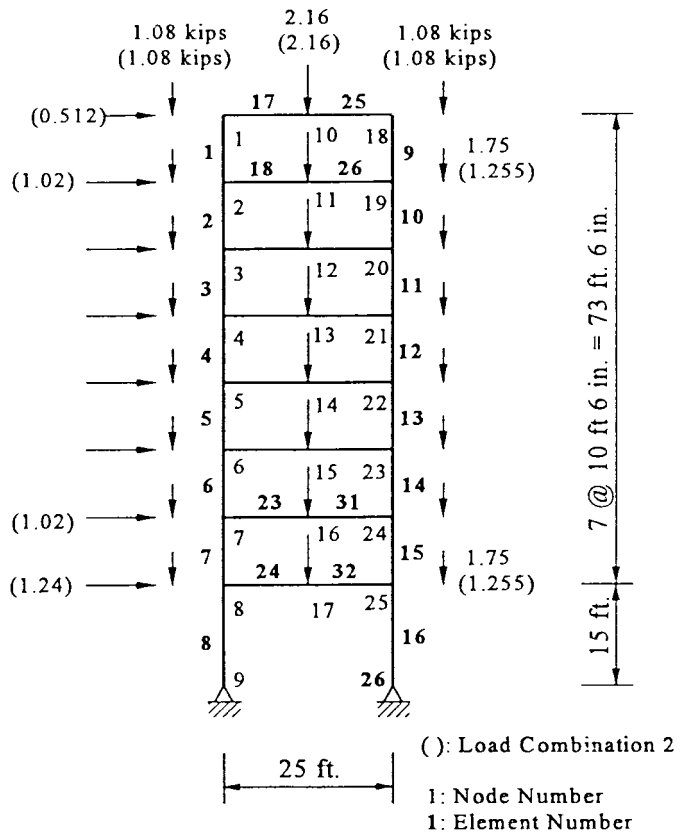


FIGURE 28.42: Structural modeling of the eight-story frame.

concentrated lateral loads. The roof beam connections are the top and seat angles of L6x4.0x3/8x7 with double web angles of L4x3.5x1/4x5.5 made of A36 steel. The floor beam connections are the top and seat angles of L6x4x9/16x7 with double web angles of L4x3.5x5/16x8.5. All fasteners are A325 3/4-in.-diameter bolts. All members are assumed to be continuously braced laterally.

### Design by Advanced Analysis

#### Step 1: Load Condition and Preliminary Member Size

The load conditions are shown in Figure 28.44. The initial member sizes are selected as W8x21, W12x22, and W16x40 for the columns, the roof beams, and the floor beams, respectively.

#### Step 2: Structural Modeling

Each column is modeled with one element and beam with two elements. The distributed gravity loads are converted to equivalent concentrated loads on the beam, shown in Figure 28.45. In explicit imperfection modeling, the geometric imperfection is obtained by multiplying the column height by 0.002. In the equivalent notional load method, the notional load is 0.002 times the total gravity load plus the lateral load. In the further reduced tangent modulus method, the program automatically accounts for geometric imperfection effects. Although users can choose any of these three models, the further reduced tangent modulus model is the only one presented herein. The incremental loads are computed by dividing the concentrated load by the scaling factor of 20.

#### Step 3: Analysis

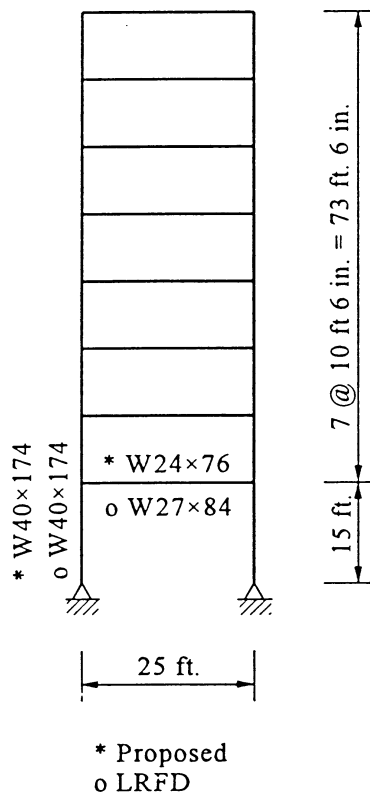


FIGURE 28.43: Comparison of member sizes of the eight-story frame.

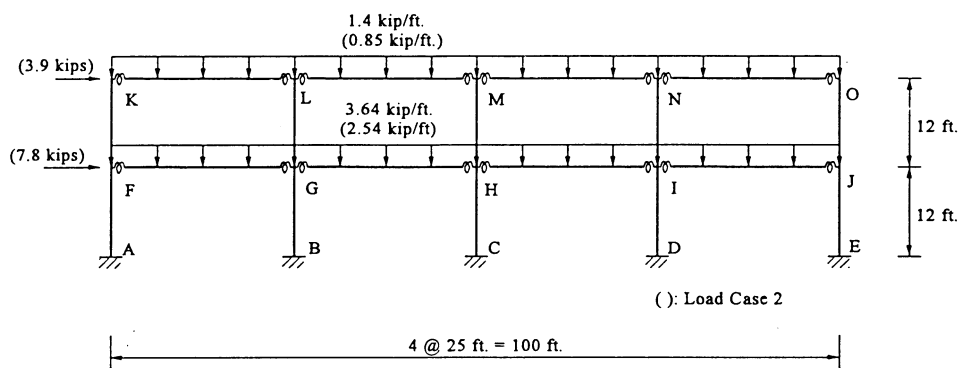


FIGURE 28.44: Configuration and load condition of two-story four-bay semi-rigid frame.

The three parameters of the connections can be computed by use of the computer program 3PARA. Corresponding to the input format in Table 28.2, the input data, CONN.DAT, may be generated, as shown in Tables 28.10a and 28.10b.

Referring to the input instructions (Section 28.5.4), the input data is written in the form shown in Tables 28.11a and 28.11b. Programs DATAGEN, INPUT, and PAAP are executed sequentially by typing "RUN." The program will continue to analyze with increasing load steps up to the ultimate

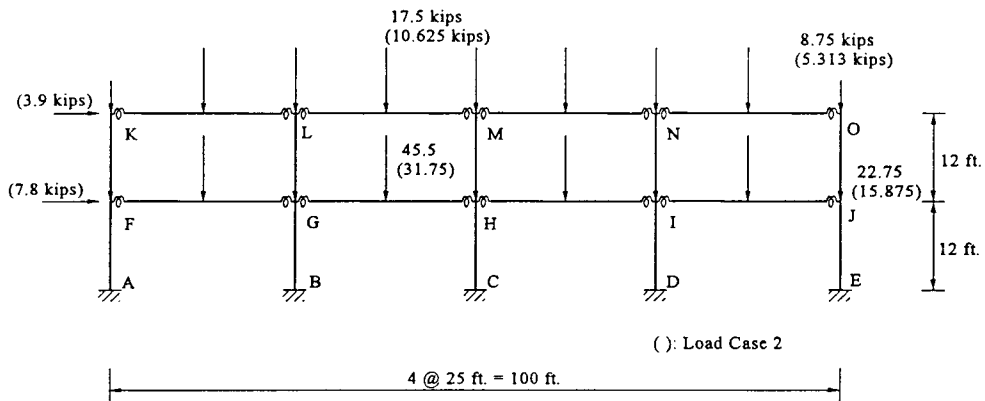


FIGURE 28.45: Concentrated load condition converted from the distributed load for the two-story one-bay semi-rigid frame.

**Table 28.10a** Input Data, CONN.DAT, of Connection for Roof Beam

2	36.0	29000			
7	0.375	0.875	2.5	1.25	12
5.5	0.25	0.6875	2.5		

**Table 28.10b** Input Data, CONN.DAT, of Connection for Floor Beam

2	36.0	29000			
7	0.5625	1.0625	2.5	1.25	16
8.5	0.3125	0.75	2.5		

state.

#### Step 4: Check of Load-Carrying Capacity

As shown in output file, P. OUT2, the ultimate load-carrying capacities of the load combinations 1 and 2 are 46.2 and 42.9 kips, respectively, at nodes 7–13 (Figure 28.45). Compared to the applied loads, 45.5 and 31.75 kips, the initial member sizes are adequate.

#### Step 5: Check of Serviceability

The lateral displacement at roof level corresponding to 1.0W is computed as 0.51 in. from the computer output, P. OUT2. The drift ratio is 1/565, which satisfies the limitation 1/400. The preliminary member sizes are satisfactory.

#### Comparison of Results

The member sizes by the advanced analysis and LRFD methods are compared in Figure 28.46. The beam members are one size larger in the advanced analysis method, and the interior columns are one size smaller.

## 28.7 Defining Terms

**Advanced analysis:** Analysis predicting directly the stability of a structural system and its component members and not needing separate member capacity checks.

**ASD:** Acronym for Allowable Stress Design.

**Beam-columns:** Structural members whose primary function is to carry axial force and bending

**Table 28.11a** Input Data, P.DAT, of the Four-Bay Two-Story Semi-Rigid Frame

Four-bay two-story semi-rigid frame (Load case 1)						
3	1					
23	5	100				
2	3	0				
16	26	0				
1	1361.0	607384.0	0.927			
2	446.0	90887.0	1.403			
1	6.16	75.3	20.4	29000.0	36.0	1
2	6.48	156.0	29.3	29000.0	36.0	
3	11.8	518.0	72.9	29000.0	36.0	
1	11	1	1			
2	12	2	1			
3	13	1	1			
4	14	2	1			
5	15	1	1			
6	16	2	1			
7	17	1	1			
8	18	2	1			
9	19	1	2			
10	20	2	2			
11	21	1	2			
12	22	2	2			
13	23	1	2			
14	24	2	2			
15	25	1	2			
16	26	2	2			
1	0.0	144.0	1	1	6	
2	0.0	144.0	1	2	8	
3	0.0	144.0	1	3	10	
4	0.0	144.0	1	4	12	
5	0.0	144.0	1	5	14	
6	0.0	144.0	1	6	15	
7	0.0	144.0	1	8	17	3
10	0.0	144.0	1	14	23	
11	150.0	0.0	3	6	7	8
19	150.0	0.0	2	15	16	8
1	1	1	1	5		
6		-1.1375				
7		-2.2750			7	
14		-1.1375				
15		-0.4375				
16		-0.8750			7	
23		-0.4375				

**Table 28.11b** Input Data, P.DAT, of the Four-Bay Two-Story Semi-Rigid Frame

Four-bay two-story semi-rigid frame (Load case 2)							
3	1						
23	5	100					
2	3	0					
16	26	0					
1	1361.0	607384.0	0.927				
2	446.0	90887.0	1.403				
1	6.16	75.3	20.4	29000.0	36.0	1	
2	6.48	156.0	29.3	29000.0	36.0		
3	11.8	518.0	72.9	29000.0	36.0		
1	11	1	1				
2	12	2	1				
3	13	1	1				
4	14	2	1				
5	15	1	1				
6	16	2	1				
7	15	1	1				
8	16	2	1				
9	19	1	2				
10	20	2	2				
11	21	1	2				
12	22	2	2				
13	23	1	2				
14	24	2	2				
15	25	1	2				
16	26	2	2				
1	0.0	144.0	1	1	6		
2	0.0	144.0	1	2	8		
3	0.0	144.0	1	3	10		
4	0.0	144.0	1	4	12		
5	0.0	144.0	1	5	14		
6	0.0	144.0	1	6	15		
7	0.0	144.0	1	8	17	3	2
10	0.0	144.0	1	14	23		
11	150.0	0.0	3	6	7	8	
19	150.0	0.0	2	15	16	8	
1	1	1	1	5			
6	0.39	-0.7938					
7		-1.5880			7		
14		-0.7938					
15	0.195	-0.2657					
16		-0.5313			7		
23		-0.2657					

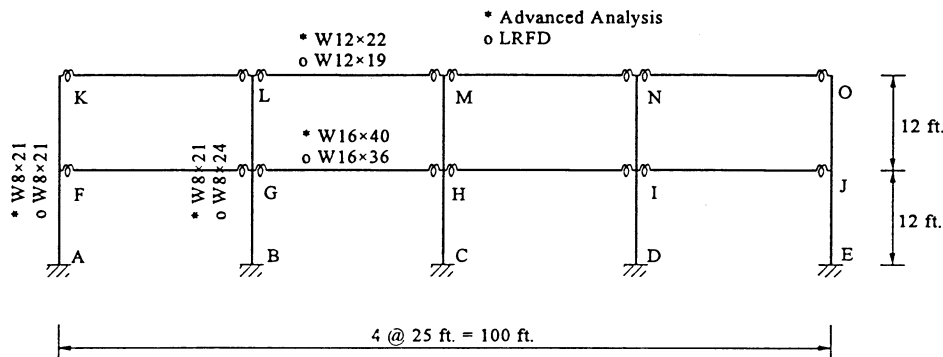


FIGURE 28.46: Comparison of member sizes of the two-story four-bay semi-rigid frame.

moment.

Braced frame: Frame in which lateral deflection is prevented by braces or a shear walls.

CRC: Acronym for Column Research Council.

Column: Structural member whose primary function is to carry axial force.

Drift: Lateral deflection of a building.

Ductility: Ability of a material to undergo a large deformation without a significant loss in strength.

Factored load: The product of the nominal load and a load factor.

Flexural member: Structural member whose primary function is to carry bending moment.

Geometric imperfection: Unavoidable geometric error during fabrication and erection.

Limit state: A condition in which a structural or structural component becomes unsafe (strength limit state) or unfit for its intended function (serviceability limit state).

Load factor: A factor to account for the unavoidable deviations of the actual load from its nominal value and uncertainties in structural analysis.

LRFD: Acronym for Load Resistance Factor Design.

Notional load: Load equivalent to geometric imperfection.

PD: Acronym for Plastic Design.

Plastic hinge: A yield section of a structural member in which the internal moment is equal to the plastic moment of the cross-section.

Plastic zone: A yield zone of a structural member in which the stress of a fiber is equal to the yield stress.

Refined plastic hinge analysis: Modified plastic hinge analysis accounting for gradual yielding of a structural member.

Resistance factors: A factor to account for the unavoidable deviations of the actual resistance of a member or a structural system from its nominal value.

Second-order analysis: Analysis to use equilibrium equations based on the deformed geometry of a structure under load.

Semi-rigid connection: Beam-to-column connection whose behavior lies between fully rigid and ideally pinned connection.

Service load: Nominal load under normal usage.

Stability function: Function to account for the bending stiffness reduction due to axial force.

Stiffness: Force required to produce unit displacement.

Unbraced frame: Frame in which lateral deflections are not prevented by braces or shear walls.

## References

---

- [1] Ad Hoc Committee on Serviceability. 1986. Structural Serviceability: a critical appraisal and research needs, *J. Struct. Eng.*, ASCE, 112(12), 2646-2664.
- [2] American Institute of Steel Construction. 1994. *Load and Resistance Factor Design Specification*, 2nd ed., Chicago.
- [3] American Institute of Steel Construction. 1986. *Load and Resistance Factor Design Specification for Structural Steel Buildings*, Chicago.
- [4] Canadian Standard Association. 1994. *Limit States Design of Steel Structures*, CAN/CSA-S16.1-M94.
- [5] Canadian Standard Association. 1989. *Limit States Design of Steel Structures*, CAN/CSA-S16.1-M89.
- [6] Chen, W. F. and Kim, S. E. 1997. *LRFD Steel Design Using Advanced Analysis*, CRC Press, Boca Raton, FL.
- [7] Chen, W. F. and Lui, E. M. 1992. *Stability Design of Steel Frames*, CRC Press, Boca Raton, FL.
- [8] Chen, W.F. and Lui, E.M. 1986. *Structural Stability—Theory and Implementation*, Elsevier, New York.
- [9] Cook, R.D., Malkus, D.S., and Plesha, M.E. 1989. *Concepts and Applications of Finite Element Analysis*, 3rd ed., John Wiley & Sons, New York.
- [10] ECCS. 1991. *Essentials of Eurocode 3 Design Manual for Steel Structures in Building*, ECCS-Advisory Committee 5, No. 65.
- [11] ECCS. 1984. *Ultimate Limit State Calculation of Sway Frames with Rigid Joints*, Technical Committee 8—Structural Stability Technical Working Group 8.2— System, Publication No. 33.
- [12] Ellingwood. 1989. Serviceability Guidelines for Steel Structures, *Eng. J.*, AISC, 26, 1st Quarter, pp. 1-8.
- [13] Hughes, T. J. R. 1987. *The Finite Element Method: Linear Static and Dynamic Finite Element Analysis*, Prentice-Hall, Englewood Cliffs, NJ.
- [14] Kanchanalai, T. 1977. The Design and Behavior of Beam-Columns in Unbraced Steel Frames, AISI Project No. 189, Report No. 2, Civil Engineering/Structures Research Lab., University of Texas at Austin.
- [15] Kim, S.E. 1996. Practical Advanced Analysis for Steel Frame Design, Ph.D. thesis, School of Civil Engineering, Purdue University, West Lafayette, IN.
- [16] Kim, S. E. and Chen, W. F. 1996. Practical advanced analysis for steel frame design, *ASCE Structural Congress XIV*, Chicago, Special Proceeding Volume on Analysis and Computation, April, pp. 19-30.
- [17] Kim, S. E. and Chen, W. F. 1996. Practical advanced analysis for braced steel frame design, *J. Struct. Eng.*, ASCE, 122(11), 1266-1274.
- [18] Kim, S. E. and Chen, W. F. 1996. Practical advanced analysis for unbraced steel frame design, *J. Struct. Eng.*, ASCE, 122(11), 1259-1265.
- [19] Kim, S. E. and Chen, W. F. 1996. Practical advanced analysis for semi-rigid frame design, *AISC Eng. J.*, 33(4), 129-141.
- [20] Kim, S. E. and Chen, W. F. 1996. Practical advanced analysis for frame design—Case study, *SSSS J.*, 6(1), 61-73.

- [21] Kish, N. and Chen, W. F. 1990. Moment-rotation relations of semi-rigid connections with angles, *J. Struct. Eng.*, ASCE, 116(7), 1813-1834.
- [22] Kishi, N., Goto, Y., Chen, W. F., and Matsuoka, K. G. 1993. Design aid of semi-rigid connections for frame analysis, *Eng. J.*, AISC, 4th quarter, pp. 90-107.
- [23] LeMessurier, W. J. 1977. A practical method of second order analysis, Part 2—Rigid frames. *AISC Eng. J.*, 14(2), 49-67.
- [24] Liew, J. Y. R. 1992. Advanced Analysis for Frame Design, Ph.D. thesis, School of Civil Engineering, Purdue University, West Lafayette, IN.
- [25] Liew, J. Y. R., White, D. W., and Chen, W. F. 1993. Second-order refined plastic hinge analysis of frame design: Part I, *J. Struct. Eng.*, ASCE, 119(11), 3196-3216.
- [26] Liew, J. Y. R., White, D. W., and Chen, W. F. 1993. Second-order refined plastic-hinge analysis for frame design: Part 2, *J. Struct. Eng.*, ASCE, 119(11), 3217-3237.
- [27] Maleck, A. E., White, D. W., and Chen, W. F. 1995. Practical application of advanced analysis in steel design, *Proc. 4th Pacific Structural Steel Conf.*, Vol. 1, Steel Structures, pp. 119-126.
- [28] SSRC 1981. General principles for the stability design of metal structures, Technical Memorandum No. 5, Civil Engineering, ASCE, February, 53-54.
- [29] White, D. W. and Chen, W. F., Eds., 1993. *Plastic Hinge Based Methods for Advanced Analysis and Design of Steel Frames: An Assessment of the State-of-the-art*, SSRC, Lehigh University, Bethlehem, PA.
- [30] Standards Australia. 1990. *AS4100-1990, Steel Structures*, Sydney, Australia.
- [31] Stelmack T. W. 1982. Analytical and Experimental Response of Flexibly-Connected Steel Frames, M.S. dissertation, Department of Civil, Environmental, and Architectural Engineering, University of Colorado.
- [32] Vogel, U. 1985. Calibrating frames, *Stahlbau*, 10, 1-7.
- [33] White, D. W. 1993. Plastic hinge methods for advanced analysis of steel frames, *J. Constr. Steel Res.*, 24(2), 121-152.

## Further Reading

---

- [1] Chen, W. F. and Kim, S. E. 1997. *LRFD Steel Design Using Advanced Analysis*, CRC Press, Boca Raton, FL.
- [2] Chen, W. F. and Lui, E. M. 1992. *Stability Design of Steel Frames*, CRC Press, Boca Raton, FL.
- [3] Chen, W. F. and Toma, S. 1994. *Advanced Analysis of Steel Frames*, CRC Press, Boca Raton, FL.
- [4] Chen, W. F. and Sohal, I. 1995. *Plastic Design and Second-Order Analysis of Steel Frames*, Springer-Verlag, New York.
- [5] Chen, W. F., Goto, Y., and Liew, J. Y. R. 1996. *Stability Design of Semi-Rigid Frames*, John Wiley & Sons, New York.